of mdx-23 mice at 7 days, 3 weeks, 2 months, 4 months and 7 months of age ($n = 3$ per age group). Serum samples from 7-day-, 5-week- and 2-month-old BL10 mice were used as controls. Each serum sample containing 50 μg total protein was spiked with ^{15}N-labeled BL6 serum aliquots containing 25 μg total proteins. We have chosen to spike at 2:1 ratio to minimize the usage of ^{15}N labeled serum stock.

Each spiked sample was further fractionated by SDS–PAGE using 4–12% Bis Tris HCl pre-cast gels (Invitrogen Life Technologies, Grand Island, NY, USA). The gel was then stained with Bio-Safe Coomassie (Bio-Rad, Hercules, CA, USA) and each lane was cut into 20–30 bands. Each band was then in-gel digested using trypsin (Promega, Madison, WI, USA), and the resulting peptides were extracted and analyzed by nano-LC-MS/MS as described below.

Peptide mixtures from each band were resuspended in 10 μl of 0.1% formic acid and loaded (6 μl) via an auto-sampler onto a Symmetry C18 trap column (5 μm, 300 μm inner diameter × 23 mm, Waters Milford, MA, USA). The trapped peptides were washed for 10 min with 0.1% formic acid at a flow rate of 10 μl/min and then eluted on a C18 reversed-phase column (3.5 μm, 75 μm × 15 cm, LC Packings, Sunnyvale, CA, USA) at a flow rate of 250 nl/min using a Nano-HPLC system from Eksigent (Dublin, CA, USA) and a mobile phase consisting of water with 0.1% formic acid (A) and 90% acetonitrile (B). A 65-min linear gradient from 5 to 40% B was employed. Eluted peptides were introduced into the mass spectrometer via a 10 μm silica tip (New Objective Inc., Ringoes, NJ, USA) adapted to a nano-electrospray source (Thermo Fisher Scientific). The spray voltage was set at 1.2 kV, and the heated capillary at 200°C. The LTQ-Orbitrap-XL (ThermoFisher Scientific) was operated in the data-dependent mode with dynamic exclusion, in which one cycle of experiments consisted of a full MS survey scan in the Orbitrap (300–2000 m/z, at 30 000 resolution) and five subsequent MS/MS scans in the LTQ of the most intense peaks, using collision-induced dissociation with helium gas and normalized collision energy value set at 35%.

Database search and SILAC ratio measurement

Protein identification and quantification were performed using the IP2 software version 1.01 (Integrated Proteomics Applications, San Diego, CA, USA). Files from each lane were searched against the forward and reverse Uniprot mouse database (UniProt release 15.15, January 2013, 16 580 forward entries) for partially tryptic peptides, allowing two missed cleavages and the possible modifications of Met residue by oxidation (+15.99492 Da), of Lys residue (+6.0204 Da) in the case of $^{13}C_6$-Lys spike-in strategy and nitrogen atom (+0.98 Da) in the case of ^{15}N spike-in strategy. IP2 uses the Sequest search engine version 2010 (06 10 13 1836). The mass tolerance was set at ± 30 ppm ($^{13}C_6$-Lys) or ± 300 ppm (^{15}N) for MS and 1.5 Da for MS/MS. Data were filtered by setting the protein false discovery rate at <1%. Only proteins that were identified by at least two unique peptides were retained for further quantitative analysis. Census software (version 1.77), built into the IP2 platform was used to determine the ratios of light to heavy peptide pairs using an extracted chromatogram approach. Quantitative data were filtered based on a determinant value of 0.5 and an outlier P-value of 0.1.

Label-free proteome profiling of serum samples of DMD and age-matched healthy controls

Serum samples from 4, 8, 12 and 15 years old DMD patients ($n = 3$ per age group) and from 3 healthy control subjects ranging in age from 6 to 15 years were collected through the Cooperative International Neuromuscular Research Group (CINRG) network according to an approved institutional IRB protocol and used for an independent biomarker discovery experiment for human subjects. Aliquots containing 100 μg total proteins from each serum sample were further separated by SDS–PAGE and in-gel digestion as described above. The resulting peptides were extracted and analyzed by nano-LC-MS/MS using ultra-high performance liquid chromatography system, connected to a Q-Exactive Hybrid Quadrupole Orbitrap mass spectrometer (Thermo Fisher Scientific) in data-dependent top 10 mode. The generated raw files were uploaded for protein identification using the Proteome Discoverer software version 1.4.0.288 (ThermoFisher Scientific) and searched against the Uniprot human database (UniProt release 2013_07), partially tryptic peptides, 2 missed cleavages, potential modification of oxidized methionine (+15.995 Da), peptide mass tolerance of ± 10 ppm and fragment tolerance of ± 0.02 Da. Results were filtered based on the following: false discovery rate <1%, peptide probability >0.01, Delta Cn >0.1 and Xcorr > 1.5, 2, 2.25, 2.5 for z 1, 2, 3, 4. Identified proteins and peptides were exported as PepXml format and directly uploaded into ProteoIQ software version 2.3.07 (NuSep, Bogart, GA, USA) for spectral count and label-free proteome profiling. Spectral counts were normalized based on total protein spectral count.

Western blot analysis

Aliquots (containing 30 μg total protein each) from same DMD and control serum samples above with an additional three controls were further separated by SDS–PAGE as described above. Replicate gels were run to test different antibodies. Separated proteins were transferred to nitrocellulose membranes (Millipore, Billerica, MA, USA) at 300 mA for 90 min at room temperature. Membranes were blocked in TBS-T (20 mM Tris, 500 mM NaCl, pH 7.5, with 0.1% Tween 20) supplemented with 5% non-fat dry milk (Bio-Rad) for 1 h at room temperature. The membranes were then incubated overnight at 4°C with rabbit antibodies raised against the human prophosphoglycerate mutase-2 (Origene, Rockville, MD, USA), glycogen phosphorylase (Origene), myomesin-3 (Sigma Aldrich, St Louis, MO, USA) and mouse antibodies raised against human skeletal muscle myosin (Sigma Aldrich) and human filamin-C (Origene).

Each antibody was diluted in TBS-T-5% milk according to the manufacturer instruction and used to react with membrane transblots. Membranes were washed three times (for 10 min each time) in TBS-T and incubated with goat anti-rabbit or rabbit anti-mouse secondary antibodies (Dako, Carpinteria, CA, USA) conjugated to horseradish peroxidase (1:3000 in TBS-T-5% milk) for 1 h at room temperature. The protein bands were revealed with ECL chemi-luminescence substrate (Amersham Biosciences). For quantification, the X-ray films were scanned, and densitometry analysis was carried out using a Bio-Rad GS-800 calibrated densitometer running Quantity One software (Bio-Rad).

Ratios of the optical density of each specific protein to the total loaded proteins.

SUPPLEMENTARY MATERIAL

Supplementary Material is available at *HMG* online.

ACKNOWLEDGEMENTS

Authors would like to thank Lauren Hache and Zoe Sund for their help coordinating initial patient's serum collection with CINRG sites and Dr Paula Clemens for her suggestions and guidance. Authors are also thankful to DMD patients and their families for their time and efforts.

FUNDING

This work was supported by the National Institutes of Health (R01AR062380 to Y.H. and C.M.), partially by the following National Institutes of Health core grants (P50AR060836, R24HD050846, P30HD040677, UL1TR000075 to Y.H., E.H. and K.N.) and the following philanthropic funds (Board of Visitors foundation and the Lynn and Doug Parsons foundation).

REFERENCES

1. Danieli, G.A., Mostacciuolo, M.L., Bonfante, A. and Angelini, C. (1977) Duchenne muscular dystrophy. A population study. *Hum. Genet.*, **35**, 225–231.
2. Bushby, K., Finkel, R., Birnkrant, D.J., Case, L.E., Clemens, P.R., Cripe, L., Kaul, A., Kinnett, K., McDonald, C., Pandya, S. *et al.* (2009) Diagnosis and management of Duchenne muscular dystrophy, part 1: diagnosis, and pharmacological and psychosocial management. *Lancet Neurol.*, **9**, 77–93.
3. Griggs, R.C., Moxley, R.T. III, Mendell, J.R., Fenichel, G.M., Brooke, M.H., Pestronk, A. and Miller, J.P. (1991) Prednisone in Duchenne dystrophy. A randomized, controlled trial defining the time course and dose response. Clinical Investigation of Duchenne Dystrophy Group. *Arch. Neurol.*, **48**, 383–388.
4. Manzur, A.Y., Kinali, M. and Muntoni, F. (2008) Update on the management of Duchenne muscular dystrophy. *Arch. Dis. Child.*, **93**, 986–990.
5. Manzur, A.Y., Kuntzer, T., Pike, M. and Swan, A. (2008) Glucocorticoid corticosteroids for Duchenne muscular dystrophy. *Cochrane Database Syst. Rev.*, CD003725.
6. Angelini, C., Pegoraro, E., Turella, E., Intino, M.T., Pini, A. and Costa, C. (1994) Deflazacort in Duchenne dystrophy: study of long-term effect. *Muscle Nerve*, **17**, 386–391.
7. DeSilva, S., Drachman, D.B., Mellits, D. and Kuncl, R.W. (1987) Prednisone treatment in Duchenne muscular dystrophy. Long-term Benefit. *Arch. Neurol.*, **44**, 818–822.
8. McAdam, L.C., Mayo, A.L., Alman, B.A. and Biggar, W.D. (2012) The Canadian experience with long-term deflazacort treatment in Duchenne muscular dystrophy. *Acta Myol.*, **31**, 16–20.
9. Ricotti, V., Ridout, D.A., Scott, E., Quinlivan, R., Robb, S.A., Manzur, A.Y. and Muntoni, F. (2013) Long-term benefits and adverse effects of intermittent versus daily glucocorticoids in boys with Duchenne muscular dystrophy. *J. Neurol. Neurosurg. Psychiatry*, **84**, 698–705.
10. Aartsma-Rus, A., Bremmer-Bout, M., Janson, A.A., den Dunnen, J.T., van Ommen, G.J. and van Deutekom, J.C. (2002) Targeted exon skipping as a potential gene correction therapy for Duchenne muscular dystrophy. *Neuromuscul. Disord.*, **12**(Suppl. 1), S71–S77.
11. Finkel, R.S. (2010) Read-through strategies for suppression of nonsense mutations in Duchenne/Becker muscular dystrophy: aminoglycosides and ataluren (PTC124). *J. Child. Neurol.*, **25**, 1158–1164.
12. Nelson, S.F., Crosbie, R.H., Miceli, M.C. and Spencer, M.J. (2009) Emerging genetic therapies to treat Duchenne muscular dystrophy. *Curr. Opin. Neurol.*, **22**, 532–538.
13. Pichavant, C., Aartsma-Rus, A., Clemens, P.R., Davies, K.E., Dickson, G., Takeda, S., Wilton, S.D., Wolff, J.A., Wooddell, C.I., Xiao, X. *et al.* (2011) Current status of pharmaceutical and genetic therapeutic approaches to treat DMD. *Mol. Ther.*, **19**, 830–840.
14. Fairclough, R.J., Wood, M.J. and Davies, K.E. (2013) Therapy for Duchenne muscular dystrophy: renewed optimism from genetic approaches. *Nat. Rev. Genet.*, **14**, 373–378.
15. Jarmin, S., Kymalainen, H., Popplewell, L. and Dickson, G. (2014) New developments in the use of gene therapy to treat Duchenne muscular dystrophy. *Expert Opin. Biol. Ther.*, **14**, 209–230.
16. Partridge, T.A. (2011) Impending therapies for Duchenne muscular dystrophy. *Curr. Opin. Neurol.*, **24**, 415–422.
17. Cirak, S., Arechavala-Gomeza, V., Guglieri, M., Feng, L., Torelli, S., Anthony, K., Abbs, S., Garralda, M.E., Bourke, J., Wells, D.J. *et al.* (2011) Exon skipping and dystrophin restoration in patients with Duchenne muscular dystrophy after systemic phosphorodiamidate morpholino oligomer treatment: an open-label, phase 2, dose-escalation study. *Lancet*, **378**, 595–605.
18. Goemans, N.M., Tulinius, M., van den Akker, J.T., Burm, B.E., Ekhart, P.F., Heuvelmans, N., Holling, T., Janson, A.A., Platenburg, G.J., Sipkens, J.A. *et al.* (2011) Systemic administration of PRO051 in Duchenne's muscular dystrophy. *N. Engl. J. Med.*, **364**, 1513–1522.
19. Mendell, J.R., Rodino-Klapac, L.R., Sahenk, Z., Roush, K., Bird, L., Lowes, L.P., Alfano, L., Gomez, A.M., Lewis, S., Kota, J. *et al.* (2013) Eteplirsen for the treatment of Duchenne muscular dystrophy. *Ann. Neurol.*, **74**, 637–647.
20. Mendell, J.R., Rodino-Klapac, L., Sahenk, Z., Malik, V., Kaspar, B.K., Walker, C.M. and Clark, K.R. (2007) Gene therapy for muscular dystrophy: lessons learned and path forward. *Neurosci. Lett.*, **527**, 90–99.
21. Heier, C.R., Damsker, J.M., Yu, Q., Dillingham, B.C., Huynh, T., Van der Meulen, J.H., Sali, A., Miller, B.K., Phadke, A., Scheffer, L. *et al.* (2013) VBP15, a novel anti-inflammatory and membrane-stabilizer, improves muscular dystrophy without side effects. *EMBO Mol. Med.*, **5**, 1569–1585.
22. McDonald, C.M., Henricson, E.K., Han, J.J., Abresch, R.T., Nicorici, A., Elfring, G.L., Atkinson, L., Reha, A., Hirawat, S. and Miller, L.L. (2009) The 6-minute walk test as a new outcome measure in Duchenne muscular dystrophy. *Muscle Nerve*, **41**, 500–510.
23. Mazzone, E.S., Messina, S., Vasco, G., Main, M., Eagle, M., D'Amico, A., Doglio, L., Politano, L., Cavallaro, F., Frosini, S. *et al.* (2009) Reliability of the North Star Ambulatory Assessment in a multicentric setting. *Neuromuscul. Disord.*, **19**, 458–461.
24. Scott, E., Eagle, M., Mayhew, A., Freeman, J., Main, M., Sheehan, J., Manzur, A. and Muntoni, F. (2012) Development of a functional assessment scale for ambulatory boys with Duchenne muscular dystrophy. *Physiother. Res. Int.*, **17**, 101–109.
25. Escolar, D.M., Hache, L.P., Clemens, P.R., Cnaan, A., McDonald, C.M., Viswanathan, V., Kornberg, A.J., Bertorini, T.E., Nevo, Y., Lotze, T. *et al.* (2011) Randomized, blinded trial of weekend vs daily prednisone in Duchenne muscular dystrophy. *Neurology*, **77**, 444–452.
26. Okinaka, S., Kumagai, H., Ebashi, S., Sugita, H., Momoi, H., Toyokura, Y. and Fujie, Y. (1961) Serum creatine phosphokinase. Activity in progressive muscular dystrophy and neuromuscular diseases. *Arch. Neurol.*, **4**, 520–525.
27. Ohlendieck, K. (2013) Proteomic identification of biomarkers of skeletal muscle disorders. *Biomark. Med.*, **7**, 169–186.
28. Cacchiarelli, D., Legnini, I., Martone, J., Cazzella, V., D'Amico, A., Bertini, E. and Bozzoni, I. (2011) miRNAs as serum biomarkers for Duchenne muscular dystrophy. *EMBO Mol. Med.*, **3**, 258–265.
29. Mizuno, H., Nakamura, A., Aoki, Y., Ito, N., Kishi, S., Yamamoto, K., Sekiguchi, M., Takeda, S. and Hashido, K. (2011) Identification of muscle-specific microRNAs in serum of muscular dystrophy animal models: promising novel blood-based markers for muscular dystrophy. *PLoS ONE*, **6**, e18388.
30. Zaharieva, I.T., Calissano, M., Scoto, M., Preston, M., Cirak, S., Feng, L., Collins, J., Kole, R., Guglieri, M., Straub, V. *et al.* (2013) Dystromirs as serum biomarkers for monitoring the disease severity in Duchenne muscular Dystrophy. *PLoS ONE*, **8**, e80263.
31. Nadarajah, V.D., van Putten, M., Chaouch, A., Garrood, P., Straub, V., Lochmuller, H., Ginjaar, H.B., Aartsma-Rus, A.M., van Ommen, G.J., den Dunnen, J.T. *et al.* (2011) Serum matrix metalloproteinase-9 (MMP-9) as a biomarker for monitoring disease progression in Duchenne muscular dystrophy (DMD). *Neuromuscul. Disord.*, **21**, 569–578.
32. Cynthia Martin, F., Hiller, M., Spitali, P., Oonk, S., Dalebout, H., Palmblad, M., Chaouch, A., Guglieri, M., Straub, V., Lochmuller, H. *et al.* (2014)

Fibronectin is a serum biomarker for Duchenne muscular dystrophy. *Proteomics Clin. Appl.*, **8**, 269–278.
33. McClatchy, D.B., Liao, L., Park, S.K., Xu, T., Lu, B. and Yates Iii, J.R. (2011) Differential proteomic analysis of mammalian tissues using SILAM. *PLoS ONE*, **6**, e16039.
34. Rayavarapu, S., Coley, W., Cakir, E., Jahnke, V., Takeda, S., Aoki, Y., Grodish-Dressman, H., Jaiswal, J.K., Hoffman, E.P., Brown, K.J. *et al.* (2013) Identification of disease specific pathways using in vivo SILAC proteomics in dystrophin deficient mdx mouse. *Mol. Cell Proteomics*, **12**, 1061–1073.
35. Cullen, M.J. and Jaros, E. (1988) Ultrastructure of the skeletal muscle in the X chromosome-linked dystrophic (mdx) mouse. Comparison with Duchenne muscular dystrophy. *Acta Neuropathol.*, **77**, 69–81.
36. Nicholson, L.V. (1981) Serum myoglobin in muscular dystrophy and carrier detection. *J. Neurol. Sci.*, **51**, 411–426.
37. Ohta, M., Itagaki, Y., Itoh, N., Hayashi, K., Nishitani, H. and Ohta, K. (1991) Carbonic anhydrase III in serum in muscular dystrophy and other neurological disorders: relationship with creatine kinase. *Clin. Chem.*, **37**, 36–39.
38. McArdle, A., Edwards, R.H. and Jackson, M.J. (1994) Time course of changes in plasma membrane permeability in the dystrophin-deficient mdx mouse. *Muscle Nerve*, **17**, 1378–1384.
39. Matsumura, T., Saito, T., Fujimura, H. and Shinno, S. (2007) Cardiac troponin I for accurate evaluation of cardiac status in myopathic patients. *Brain Dev.*, **29**, 496–501.
40. Saito, T., Takenaka, M., Miyai, I., Yamamoto, Y., Matsumura, T., Nozaki, S. and Kang, J. (2001) Coagulation and fibrinolysis disorder in muscular dystrophy. *Muscle Nerve*, **24**, 399–402.
41. Colussi, C., Banfi, C., Brioschi, M., Tremoli, E., Straino, S., Spallota, F., Mai, A., Rotili, D., Capogrossi, M.C. and Gaetano, C. (2010) Proteomic profile of differentially expressed plasma proteins from dystrophic mice and following suberoylanilide hydroxamic acid treatment. *Proteomics Clin. Appl.*, **4**, 71–83.
42. Davalos, D. and Akassoglou, K. (2012) Fibrinogen as a key regulator of inflammation in disease. *Semin. Immunopathol.*, **34**, 43–62.
43. Vidal, B., Ardite, E., Suelves, M., Ruiz-Bonilla, V., Janue, A., Flick, M.J., Degen, J.L., Serrano, A.L. and Munoz-Canoves, P. (2012) Amelioration of Duchenne muscular dystrophy in mdx mice by elimination of matrix-associated fibrin-driven inflammation coupled to the alphaMbeta2 leukocyte integrin receptor. *Hum. Mol. Genet.*, **21**, 1989–2004.
44. Lo, A.S., Liew, C.T., Ngai, S.M., Tsui, S.K., Fung, K.P., Lee, C.Y. and Waye, M.M. (2005) Developmental regulation and cellular distribution of human cytosolic malate dehydrogenase (MDH1). *J. Cell. Biochem.*, **94**, 763–773.
45. Minarik, P., Tomaskova, N., Kollarova, M. and Antalik, M. (2002) Malate dehydrogenases—structure and function. *Gen. Physiol. Biophys.*, **21**, 257–265.
46. Chen, Y.W., Zhao, P., Borup, R. and Hoffman, E.P. (2000) Expression profiling in the muscular dystrophies: identification of novel aspects of molecular pathophysiology. *J. Cell. Biol.*, **151**, 1321–1336.
47. Frolova, E.G., Sopko, N., Blech, L., Popovic, Z.B., Li, J., Vasanji, A., Drumm, C., Krukovets, I., Jain, M.K., Penn, M.S. *et al.* (2012) Thrombospondin-4 regulates fibrosis and remodeling of the myocardium in response to pressure overload. *FASEB J.*, **26**, 2363–2373.
48. Diez, J.J. and Iglesias, P. (2003) The role of the novel adipocyte-derived hormone adiponectin in human disease. *Eur. J. Endocrinol.*, **148**, 293–300.
49. Hollingsworth, K.G., Garrood, P., Eagle, M., Bushby, K. and Straub, V. (2013) Magnetic resonance imaging in Duchenne muscular dystrophy: longitudinal assessment of natural history over 18 months. *Muscle Nerve*, **48**, 586–588.
50. Hindi, S.M., Shin, J., Ogura, Y., Li, H. and Kumar, A. (2013) Matrix metalloproteinase-9 inhibition improves proliferation and engraftment of myogenic cells in dystrophic muscle of mdx mice. *PLoS ONE*, **8**, e72121.
51. Vandooren, J., Van den Steen, P.E. and Opdenakker, G. (2013) Biochemistry and molecular biology of gelatinase B or matrix metalloproteinase-9 (MMP-9): the next decade. *Crit. Rev. Biochem. Mol. Biol.*, **48**, 222–272.
52. Alagaratnam, S., Mertens, B.J., Dalebout, J.C., Deelder, A.M., van Ommen, G.J., den Dunnen, J.T. and 't Hoen, P.A. (2008) Serum protein profiling in mice: identification of Factor XIIIa as a potential biomarker for muscular dystrophy. *Proteomics*, **8**, 1552–1563.
53. Chown, P.J., Barnard, E.A., Barnard, P.J., Liu, P.K. and Carter, N.D. (1984) Plasma phosphoglycerate mutase as a marker of muscular dystrophy. *J. Neurol. Sci.*, **65**, 201–210.
54. Pearson, C.M., Chowdhury, S.R., Fowler, W.M. Jr, Jones, M.H. and Griffith, W.H. (1961) Studies of enzymes in serum in muscular dystrophy. II. Diagnostic and prognostic significance in relatives of dystrophic persons. *Pediatrics*, **28**, 962–970.
55. Cohen, P., Nimmo, G.A., Burchell, A. and Antoniw, J.F. (1977) The substrate specificity and regulation of the protein phosphatases involved in the control of glycogen metabolism in mammalian skeletal muscle. *Adv. Enzyme Regul.*, **16**, 97–119.
56. Carberry, S., Brinkmeier, H., Zhang, Y., Winkler, C.K. and Ohlendieck, K. (2013) Comparative proteomic profiling of soleus, extensor digitorum longus, flexor digitorum brevis and interosseus muscles from the mdx mouse model of Duchenne muscular dystrophy. *Int. J. Mol. Med.*, **32**, 544–556.
57. Infante, J.P. and Huszagh, V.A. (1999) Mechanisms of resistance to pathogenesis in muscular dystrophies. *Mol. Cell. Biochem.*, **195**, 155–167.
58. Schoenauer, R., Lange, S., Hirschy, A., Ehler, E., Perriard, J.C. and Agarkova, I. (2008) Myomesin 3, a novel structural component of the M-band in striated muscle. *J. Mol. Biol.*, **376**, 338–351.
59. Fujita, M., Mitsuhashi, H., Isogai, S., Nakata, T., Kawakami, A., Nonaka, I., Noguchi, S., Hayashi, Y.K., Nishino, I. and Kudo, A. (2012) Filamin C plays an essential role in the maintenance of the structural integrity of cardiac and skeletal muscles, revealed by the medaka mutant zacro. *Dev. Biol.*, **361**, 79–89.
60. Bucciolini Di Sagni, M.G., Vannelli Gori, G. and Oriolo, R.A. (1982) Structural and ultrastructural changes in the skeletal muscles of patients in the early stages of Duchenne muscular dystrophy and "possible" carriers. *Boll. Soc. Ital. Biol. Sper.*, **58**, 632–638.
61. Chen, Y.W., Nagaraju, K., Bakay, M., McIntyre, O., Rawat, R., Shi, R. and Hoffman, E.P. (2005) Early onset of inflammation and later involvement of TGFbeta in Duchenne muscular dystrophy. *Neurology*, **65**, 826–834.
62. Matsumura, K., Shimizu, T., Sunada, Y., Mannen, T., Nonaka, I., Kimura, S. and Maruyama, K. (1990) Degradation of connectin (titin) in Fukuyama type congenital muscular dystrophy: immunochemical study with monoclonal antibodies. *J. Neurol. Sci.*, **98**, 155–162.
63. Rouillon, J., Zocevic, A., Leger, T., Garcia, C., Camadro, J.M., Udd, B., Wong, B., Servais, L., Voit, T. and Svinartchouk, F. (2014) Proteomics profiling of urine reveals specific titin fragments as biomarkers of Duchenne muscular dystrophy. *Neuromuscul. Disord.* Epub ahead of print.
64. Duguez, S., Duddy, W., Johnston, H., Laine, J., Le Bihan, M.C., Brown, K.J., Bigot, A., Hathout, Y., Butler-Browne, G. and Partridge, T. (2013) Dystrophin deficiency leads to disturbance of LAMP1-vesicle-associated protein secretion. *Cell. Mol. Life Sci.*, **70**, 2159–2174.
65. Araki, E., Nakamura, K., Nakao, K., Kameya, S., Kobayashi, O., Nonaka, I., Kobayashi, T. and Katsuki, M. (1997) Targeted disruption of exon 52 in the mouse dystrophin gene induced muscle degeneration similar to that observed in Duchenne muscular dystrophy. *Biochem. Biophys. Res. Commun.*, **238**, 492–497.

Environ Health Prev Med
DOI 10.1007/s12199-014-0405-7

SHORT COMMUNICATION

Three novel serum biomarkers, miR-1, miR-133a, and miR-206 for Limb-girdle muscular dystrophy, Facioscapulohumeral muscular dystrophy, and Becker muscular dystrophy

Yasunari Matsuzaka · Soichiro Kishi · Yoshitsugu Aoki · Hirofumi Komaki · Yasushi Oya · Shin-ichi Takeda · Kazuo Hashido

Received: 15 April 2014 / Accepted: 12 August 2014

Abstract
Objectives Muscular dystrophies are a clinically and genetically heterogeneous group of inherited myogenic disorders. In clinical tests for these diseases, creatine kinase (CK) is generally used as diagnostic blood-based biomarker. However, because CK levels can be altered by various other factors, such as vigorous exercise, etc., false positive is observed. Therefore, three microRNAs (miRNAs), miR-1, miR-133a, and miR-206, were previously reported as alternative biomarkers for duchenne muscular dystrophy (DMD). However, no alternative biomarkers have been established for the other muscular dystrophies.
Methods We, therefore, evaluated whether these miR-1, miR-133a, and miR-206 can be used as powerful biomarkers using the serum from muscular dystrophy patients including DMD, myotonic dystrophy 1 (DM1), limb-girdle muscular dystrophy (LGMD), facioscapulohumeral muscular dystrophy (FSHD), becker muscular dystrophy (BMD), and distal myopathy with rimmed vacuoles (DMRV) by qualitative polymerase chain reaction (PCR) amplification assay.
Results Statistical analysis indicated that all these miRNA levels in serum represented no significant differences between all muscle disorders examined in this study and controls by Bonferroni correction. However, some of these indicated significant differences without correction for testing multiple diseases ($P < 0.05$). The median values of miR-1 levels in the serum of patients with LGMD, FSHD, and BMD were approximately 5.5, 3.3 and 1.7 compared to that in controls, 0.68, respectively. Similarly, those of miR-133a and miR-206 levels in the serum of BMD patients were about 2.5 and 2.1 compared to those in controls, 1.03 and 1.32, respectively.
Conclusions Taken together, our data demonstrate that levels of miR-1, miR-133a, and miR-206 in serum of BMD and miR-1 in sera of LGMD and FSHD patients showed no significant differences compared with those of controls by Bonferroni correction. However, the results might need increase in sample sizes to evaluate these three miRNAs as variable biomarkers.

Y. Matsuzaka, S. Kishi contributed equally to this work.

Electronic supplementary material The online version of this article (doi:10.1007/s12199-014-0405-7) contains supplementary material, which is available to authorized users.

Y. Matsuzaka · S. Kishi · K. Hashido (✉)
Administrative Section of Radiation Protection, National Institute of Neuroscience, Tokyo, Japan
e-mail: hashido@ncnp.go.jp

Present Address:
S. Kishi
Department of Pathology, Institute for Developmental Research, Kasugai, Aichi 480-0392, Japan

Y. Aoki · S. Takeda
Department of Molecular Therapy, National Institute of Neuroscience, Tokyo, Japan

Present Address:
Y. Aoki
Department of Physiology, Anatomy and Genetics, University of Oxford, South Parks Road, Oxford OX1 3QX, UK

H. Komaki
Department of Child Neurology, National Center of Neurology and Psychiatry (NCNP), Kodaira, Tokyo, Japan

Y. Oya
Department of Neurology, National Center of Neurology and Psychiatry (NCNP), Kodaira, Tokyo, Japan

Published online: 24 August 2014

Keywords microRNAs · Biomarker · Limb-girdle muscular dystrophy · Facioscapulohumeral muscular dystrophy · Becker muscular dystrophy

Introduction

miRNAs are approximately 19–23 nucleotides' long single-stranded non-coding RNAs, and the function is post-transcriptional regulation of target messenger RNAs (mRNAs) [1] dysregulation of miRNAs expression in skeletal muscle and myocardium is associated with muscle disorders [2, 3]. Interestingly, despite the high RNase activity within the circulating blood, a high concentration of these remarkably stable miRNAs has been found in various body fluids, including serum and plasma, as microvesicle-encapsulated [4] or RNA-binding protein-associated forms [5].

Muscular dystrophies are classified in accordance with their clinical and pathological features [6, 7]. Among them, DMD (OMIM310200) and BMD (OMIM 300376) are caused by various mutations in the *dystrophin* gene on the X chromosome, at Xp21.2 [8], and exhibit estimated prevalences of approximately one per 3,500 in DMD and 3–6 per 100,000 in BMD [9]. DM1 (OMIM160900), also known as Steinert's disease, represents an estimated prevalence of 5.5 per 100,000 Japanese [10], and is caused by expansion of a CTG repeat in the 3′ UTR of the DMPK (dystrophia myotonica-protein kinase) gene [11]. LGMD is caused by a total of twenty-two autosomal dominant or recessive causative gene mutations [12], and has an incidence of about one per 20,000 individuals. FSHD (OMIM158900) is caused by a loss of the D4Z4 microsatellite locus on chromosome 4 [13] with a prevalence of approximately one per 20,000 Japanese [6]. DMRV (OMIM605820), also called Nonaka myopathy, hereditary inclusion body myopathy (hiBM), and quadriceps sparing myopathy, is an autosomal recessive vacuolar myopathy of the distal muscles of the tibialis anterior, caused by mutations in the UDP-N-acetylglucosamine 2-epimerase/N-acetylmannosamine kinase (GNE) gene [14]. The prevalence of DMRV is approximately 300–400 patients within the Japanese population.

Serum CK values are commonly used as clinical blood-based biomarkers for these muscular dystrophies. However, there are some problems in using serum CK values for diagnostic evaluation of these disorders, i.e. CK levels are increased by vigorous exercise [15], decreased renal function due to aging, gender-dependent differences in skeletal muscle mass, pregnancy, and alcohol intake, and does not parallel motor ability in DMD [16, 17]. We, therefore, previously reported that three miRNAs, miR-1, miR-133a, and miR-206, in the serum were used as novel biomarkers in the dystrophin-deficient muscular dystrophy mouse models, as well as the canine X-linked muscular dystrophy in Japan dog (CXMDj) [18]. Furthermore, another group reported that an increase in miR-1, miR-133a, and miR-206 levels in the serum of DMD children patients was correlated with motor ability [17]. In other muscle diseases, however, stable and valuable biomarkers as an alternative to CK have not been established to date.

In this study, we measured and evaluated these three miRNAs, miR-1, miR-133a, and miR-206, in serum as possible stable and powerful biomarkers for DM1, LGMD, LGMAD2B, FSHD, BMD, and DMRV.

Materials and methods

Patients

A total of forty-eight unrelated Japanese patients with DMD, DM1, LGMD, LGMD2B, FSHD, BMD, and DMRV and each of the five age-matched controls were enrolled in this study (Table 1). DMD patients were divided into two groups by age (average ages and age ranges were 10.2 and 28.7 years of age, 5–18 and 27–31 years of age, respectively). LGMD patients were divided into two groups by whether they contained LGMD2B or not. Informed consent was obtained from the cases and controls by explaining the details of this study prior to collection of peripheral blood. The Research Ethics Committee for National Institute of Neuroscience, National Center of Neurology and Psychiatry approved the present study and all participants provided written informed consent.

Animals

All animals used in this study were housed in the National Center of Neurology and Psychiatry and treated in accordance with the guidelines provided by the Ethics Committee for the Treatment of Laboratory Animals of National Institute of Neuroscience, or the Ethics Committee for the Treatment of Laboratory Middle-sized Animals of National Institute of Neuroscience, which has adopted the three fundamental principles of replacement, reduction, and refinement.

RNA extraction and quantification of miRNA

Total RNA was extracted from 50 μl of serum using the mirVana miRNA isolation kit (Ambion, Austin, TX, USA) according to the manufacturer's protocol and 50 μl of RNA eluate. Five μl of the RNA elute was reverse transcribed

Table 1 Muscle dystrophy patients

Disease	Sample no.	Average of age ± SD (y.a.)	Sex (male/female)	Sporadic/Familial	Average of onset ± SD (y.a.)	Serum CK (U/ml)
DMD	5	10.4 ± 4.2	5/0	3/2	3.8 ± 1.1	9,101 ± 6,282
DMD	7	28.7 ± 1.5	7/0	7/0	3.8 ± 0.7	220 ± 126
DM1	8	59.4 ± 17.4	5/3	4/4	18.4 ± 16.9	121 ± 66
LGMD	7	50.0 ± 19.8	5/2	5/2	15.5 ± 13.9	633 ± 661
LGMAD2B	4	51.0 ± 18.2	3/1	4/0	23.0 ± 5.7	2,713 ± 2,722
FSHD	8	52.3 ± 17.3	4/4	4/4	14.4 ± 10.8	162 ± 155
BMD	4	52.0 ± 12.9	4/0	4/0	14 ± 14.6	687 ± 562
DMRV	5	39.2 ± 7.3	0/4	4/1	22.2 ± 6.2	206 ± 177

y.a years of age

using the TaqMan miRNA Reverse Transcription kit (ABI, Foster City, CA, USA) and miRNA-specific stem-loop primers (part of TaqMan miRNA assay kit: Applied Biosystems) as previously reported [18]. For exosome and exosome-depleted supernatant, 5-fold diluted solutions of the RNA elute were used with distilled water. The expression levels of miRNA were quantified by real-time PCR using individual miRNA-specific primers (part of TaqMan miRNA assay kit: Applied Biosystems) with 7900HT Fast Real-Time PCR System (Applied Biosystems) according to the manufacture's protocol. Each samples were performed real-time PCR as triplicade. Each miRNA expression was represented relative to the expression of miR-16 used as an internal control. Data analysis was performed by SDS 2.1 real-time PCR data analysis software (Applied Biosystems). Expression data were given as median values obtained from three samples in conjunction with standard deviation. Statistical comparisons were performed by Mann–Whitney *U* test. Bonferroni correction was used to resolve a problem of multiple testing.

Creatine kinase activity

Serum creatine kinase (CK) levels were measured with the Fuji Dri-chem system (Fuji Film Medical Co. Ltd, Tokyo, Japan) according to the manufacture's protocol. Ten ml of serum was deposited on a Fuji Dri-chem slide and incubated at 37 °C. The increase in absorbance by the generated dye was measured for 5 min at 540 nm spectrophotometrically, and the activity was calculated according to the installed formula. Data were expressed as units per liter (U/l).

Exosome purification

Serum was harvested from the peripheral blood of DMD patients in tubes by centrifugation at 3,000×*g* for 15 min. Isolation of exosome from serum was performed by Exo Quick Exosome Precipitation Solution (System Biosciences, CA) according to the protocol provided by the manufacturer. Briefly, 63 μl of the Exo Quick Exosome Precipitation Solution was added to 250 μl of serum. The mixture was vortexed for 15 s and then incubated at 4 °C for 30 min. After centrifugation at 1,500×*g* for 30 min at room temperature, the supernatant was discarded. Again, the centrifugation and aspiration were repeated. The pellet including exosomes was resuspended in 1× phosphate-buffered saline (PBS).

CTX-induced skeletal muscle regeneration of mice

C57Bl/10SnSlc mice were obtained from Clea Japan Inc., and used at 7–8 weeks age. Hair from the bilateral hind limbs of diethyl ether-anesthetized animals was removed with a depilatory cream before the induction of injury. The tibialis anterior (TA) muscle of mice was injured by injection of 100 μl of PBS or cardiotoxin (CTX, 10 μM) (*Naja mossambica mossambica*, Sigma-Aldrich), a snake venom that selectively injures myofibers by disturbing calcium homeostasis at the neuromuscular junctions, followed by necrosis of muscle fibers [19]. The concentration of cardiotoxin ensures minimal damage to satellite cells and also to the nerves and blood vessels of the original muscles [20]. After 1, 3, and 5 days, whole body blood was collected from the abdominal aorta under anesthesia, and allowed to stand for about 30 min at room temperature before centrifugation at 1,200×*g* for 10 min at room temperature. The supernatant was used as serum to isolate miRNAs.

Results

miRNA levels in the serum of patients of various muscle diseases

To assess the validity of miRNAs as alternative serum biomarkers to CK for various muscle diseases, we analyzed the expression levels of three miRNAs, miR-1, miR-133a,

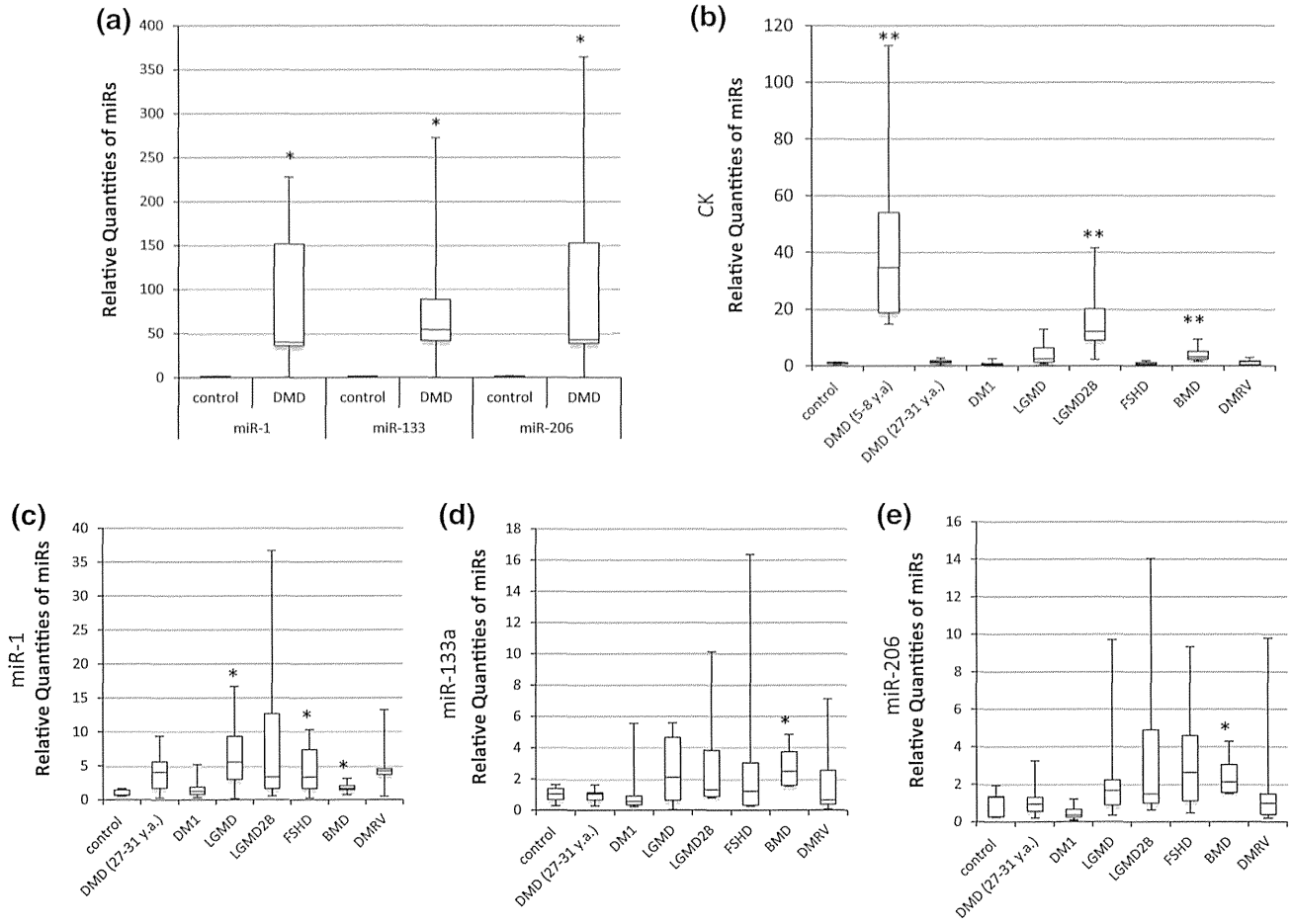

Fig. 1 Evaluation of miRNA levels in various muscular dystrophies indicated by *box plot*. **a** Expression levels of miR-1, miR-133a, and miR-206 in the serum of DMD (5–18 years of age) versus control children, evaluated by RT-pPCR. **b** CK activities in various muscular dystrophies. Expression levels of **c** miR-1, **d** miR-133a, and **e** miR-206 were examined using serum from patients with the indicated muscular dystrophies. Each *bar* represents mean ± SD. $^*P < 0.05$ versus control by Mann–Whitney *U* test

and miR-206, in DMD (5–18 and 27–31 years of age), DM1, LGMD, LGMD2B, FSHD, BMD, and DMRV patients and healthy controls. Although all these miRNA levels in sera of all muscle diseases tested in this study represented no significant differences with controls by Bonferroni correction, associations of these miRNA levels with some disorders of them were observed without multiple corrections. As previous reported, qRT-PCR showed that the median values of levels of all three miRNAs, miR-1, miR-133a, and miR-206, in the serum of DMD (5–18 years of age) were approximately 39.8, 54.0, and 43.0 compared with those of controls, 0.68, 1.03, and 1.32, respectively ($P < 0.05$, Fig. 1a). The median value of CK activity in the serum of DMD (5–18 years of age) was significantly increased compared with controls (cases verses controls; 34.6 verses 0.89, $P < 0.01$, Fig. 1b). Although LGMD2B and BMD patients also indicated high median value of CK activities compared with controls (LGMD2B, BMD verses controls; 12.1, 3.1 verses 0.89, $P < 0.05$, Fig. 1b). On the other hand, each median value of miR-1 levels in the serum of LGMD, FSHD and BMD patients was significantly increased compared with controls (LGMD, FSHD and BMD verses controls; 5.5, 3.3, and 1.7 verses 0.68, $P < 0.05$, Fig. 1c). As for miR-133a and miR-206, BMD patients presented significant increases in the median value of expression levels in the serum compared to controls (cases verses controls for miR-133a and miR-206; 2.49 verses 1.03, and 2.13 verses 1.32, $P < 0.05$, Fig. 1d, e). DM1 and DMRV showed no significant differences with controls for the three miRNAs. Next, we evaluated the three miRNAs as available biomarkers by receiver operating characteristics (ROC) analysis. These results indicated that area under the curve (AUC) in miR-1 displayed 0.83, 0.88, and 0.90 for LGMD, FSHD, and BMD, respectively, in spite of values below 0.8 for DMD (5–18 years of age), DM1, LGMD2B, DMRV (Supplemrntary Fig. 1a). Similarly, the AUC in miR-133a and miR-206 was 0.90 and 0.90 for BMD (Supplementary

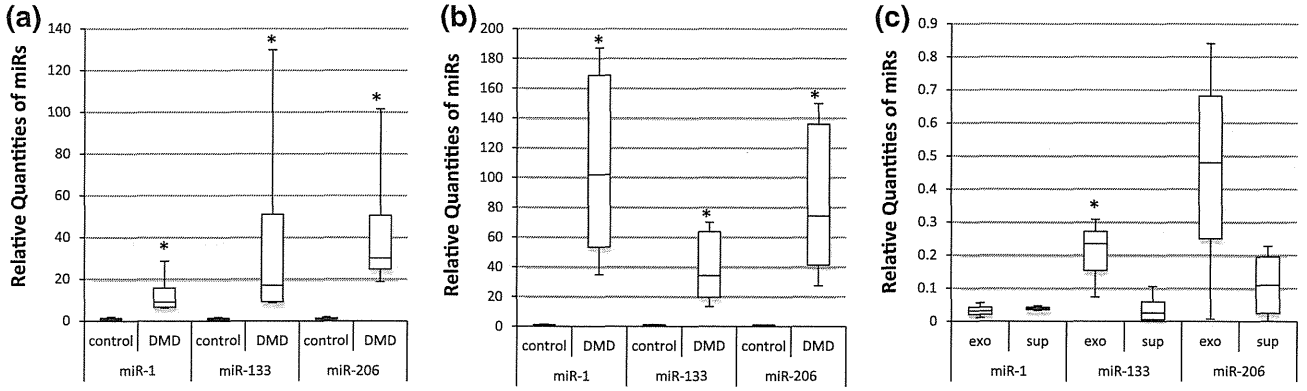

Fig. 2 Expression levels of miR-1, miR-133a, and miR-206 represented by *box plot* in (**a**) exosomes or (**b**) exosome-depleted supernatants extracted from the serum of DMD patients and controls, and analyzed by RT-qPCR. Relative expression of miR-1, miR-133a, and miR-206 is displayed as the difference in the threshold cycle number between miRNA from exosomes or the exosome-depleted supernatant extracted from the serum of DMD patients (**c**) in five times dilution. Each bar represents mean ± SD. $^*P < 0.05$ versus control by Mann–Whitney *U* test

Fig. 1b, c). miR-1 in LGMD and FSHD, and miR-1, miR-133a, and miR-206 in BMD may be useful novel biomarkers.

miRNAs expressions in exosome from the serum of DMD patients

To determine whether the up-regulation of miR-1, miR-133a, and miR-206 levels in serum of DMD patients resulted from inclusion of these miRNAs within exosome, we separated serums from patients and controls into exosome and exosome-depleted supernatant by Exo Quick Exosome Precipitation Solution. RNAs extracted from both sources were compared for the levels of the three miRNAs levels by RT-qPCR. The levels of the three miRNAs of serum of DMD patients in both fractions of exosome and exosome-depleted supernatant represented no statistically significant differences with those of controls by Bonferroni correction, but significant differences in these miRNA levels in serum between DMD patients and controls showed without multiple corrections. The median value of levels of each miR-1, miR-133a, and miR-206 in the RNAs within the exosome extracted from the DMD patients showed higher levels, 9.1, 17.0, and 30.1, compared with that of controls, 0.82, 0.77, and 0.99, respectively ($P < 0.05$, Fig. 2a). Furthermore, the median value of these miR-1, miR-133a, and miR-206 levels for RNAs from the exosome-depleted supernatant of DMD patients, 101.9, 34.1, and 74.2, exhibited high levels compared with that of controls, 1.0, 0.39, and 0.42, respectively ($P < 0.05$, Fig. 2b). To evaluate whether the majority of these miRNAs in the serum of DMD patients are concentrated in exosome or freely circulating in blood stream, the amount of the three miRNAs extracted from exosome and exosome-depleted supernatants was measured by RT-qPCR. All these miRNA levels exhibited no significant differences between exosome and exosome-depleted supernatants by Bonferroni correction. However, the levels of miR-1, miR-133a, and miR-206 in both fractions of exosome and exosome-depleted supernatant from the serum of DMD patients are remarkably increased compared with those in controls. The content of miR-133a within exosome is significantly higher than in the exosome-depleted supernatant without multiple corrections (Fig. 2c, $P < 0.05$).

miR-1, miR-133a, and miR-206 levels in mouse serum are up-regulated upon skeletal muscle regeneration

Next, to assess whether the three miRNA levels are affected in skeletal muscle regeneration in vivo, we induced skeletal muscle injury by injecting CTX into the TA of mice, and analyzed the expression of the three miRNAs by RT-qPCR at 1, 3, and 5 days after injection. The levels of miR-1, miR-133a, and miR-206 were increased dramatically by about 15-, 55-, and 15-fold in the serum of CTX-injured mice on day 1 compared with those of PBS-treated mice (Fig. 3a). However, the levels of the three miRNAs in the serum markedly decreased from day 3 to day 5 after CTX injury (Fig. 3a). On the other hand, CK activity in serum of CTX-injured mice was about 2.0-fold higher than controls between day 1 and day 3 (Fig. 3b). Our data indicate that the levels of miR-1, miR-133a, and miR-206 in serum are strikingly up-regulated by muscle injury.

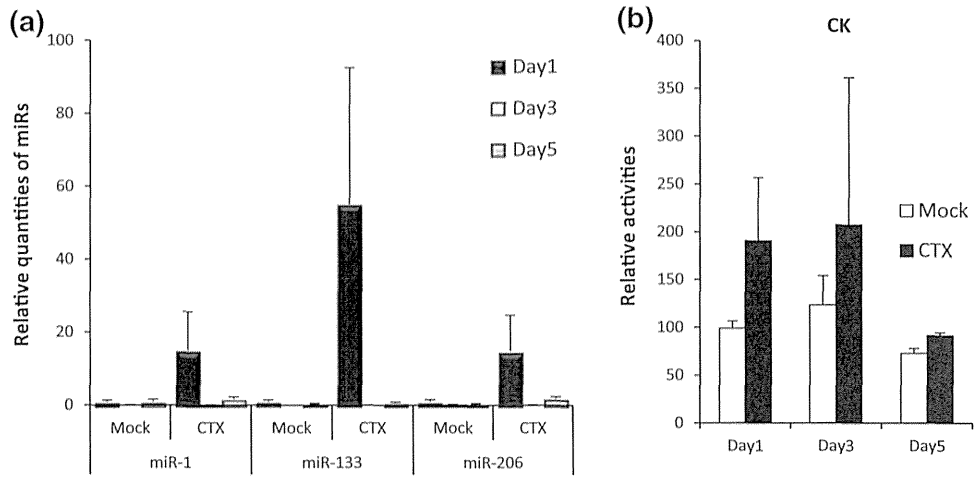

Fig. 3 **a** Expression levels of miR-1, miR-133a, and miR-206 and **b** CK activities in serum of mice on day 1, 3, and 5 after CTX ($n = 3$) injury or Mock ($n = 3$)

Discussion

In this study, miR-133a and miR-206 levels in exosome from the serum of DMD patients were increased compared to the exosome-depleted supernatant. However, it was reported that the miRNAs in *mdx* mice were more enriched in the supernatant fraction rather than in the exosome, and associated with Argonaute-2 (Ago-2) and Apolipoprotein A-1 (ApoA-1) [21]. This discrepancy may be depended on some differences for a degree of severe and progressive degeneration of affected tissues between human and mouse. It was recently reported that the miR-1, miR-133a, and miR-206 are up-regulated in both exosomes and a skeletal muscle cell line, C2C12 cells, and miRNA profiles in exosome alter during differentiation [22]. Furthermore, although the number of exosomes from C2C12 myotubes released into extracellular compartment by Dexamethasone was not changed, the abundance of the miR-1 in exosome was increased [23]. These findings represent that the up-regulations of miRNAs in serum of mice might be partly explained by their selective exports into exosomes induced by muscle degeneration and/or regeneration.

It was also reported that lack of miR-206 shows delay of muscle regeneration induced by CTX injury and more severe dystrophic phenotype in *mdx* mice due to impair differentiation of SC [24]. In our study, these miR-1, miR-133a, and miR-206 levels in the serum were up-regulated in response to CTX-induced injury. These suggested that excessive secretion of miRNAs might partly be a cause for muscle diseases.

In summary, we evaluated three miRNAs, miR-1, miR-133a, and miR-206, as novel biomarkers for muscle disorders. Although all diseases examined in this study exhibited no statistically significant associations with these miRNA levels in serum by Bonferroni correction, associations of miR-1 levels with LGMD, FSHD, and miR-133a and miR-206 with BMD showed significant differences without corrections of multiple test. However, additional studies on increasing sample size are required to further confirm its usefulness as novel biomarker for muscle disorders.

Acknowledgments We thank Dr. Jun Tanihata for valuable discussions and critical reading of the manuscript.

Conflict of interests The authors report no conflict of interests.

References

1. Esteller M. Non-coding RNAs in human disease. Nat Rev Genet. 2011;12:861–74.
2. Eisenberg I, Eran A, Nishino I, Moggio M, Lamperti C, Amato AA, et al. Distinctive patterns of microRNA expression in primary muscular disorders. Proc Natl Acad Sci U S A. 2007;104:17016–21.
3. Eisenberg I, Alexander MS, Kunkel LM. miRNAS in normal and diseased skeletal muscle. J Cell Mol Med. 2009;13:2–11.
4. Valadi H, Ekström K, Bossios A, Sjöstrand M, Lee JJ, Lötvall JO. Exosome-mediated transfer of mRNAs and microRNAs is a novel mechanism of genetic exchange between cells. Nat Cell Biol. 2007;9:654–9.
5. Yao B, Li S, Chan EK. Function of GW182 and GW bodies in siRNA and miRNA pathways. Adv Exp Med Biol. 2013;768:71–96.
6. Mercuri E, Muntoni F. Muscular dystrophies. Lancet. 2013;381:845–60.
7. Emery AE. The muscular dystrophies. Lancet. 2002;359:687–95.
8. Takeshima Y, Yagi M, Okizuka Y, Awano H, Zhang Z, Yamauchi Y, et al. Mutation spectrum of the dystrophin gene in 442 Duchenne/Becker muscular dystrophy cases from one Japanese referral center. J Hum Genet. 2010;55:379–88.
9. Tsukamoto H, Inui K, Fukushima H, Nishigaki T, Taniike M, Tanaka J, et al. Molecular study of Duchenne and Becker muscular dystrophies in Japanese. J Inherit Metab Dis. 1991;14:819–24.

10. Yamagata H, Miki T, Sakoda S, Yamanaka N, Davies J, Shelbourne P, et al. Detection of a premutation in Japanese myotonic dystrophy. Hum Mol Genet. 1994;3:819–20.
11. Udd B, Krahe R. The myotonic dystrophies: molecular, clinical, and therapeutic challenges. Lancet Neurol. 2012;11:891–905.
12. Mitsuhashi S, Kang PB. Update on the genetics of limb girdle muscular dystrophy. Semin Pediatr Neurol. 2012;19:211–8.
13. van Deutekom JC, Wijmenga C, van Tienhoven EA, Gruter AM, Hewitt JE, Padberg GW, et al. FSHD associated DNA rearrangements are due to deletions of integral copies of a 3.2 kb tandemly repeated unit. Hum Mol Genet. 1993;2:2037–42.
14. Ikeda-Sakai Y, Manabe Y, Fujii D, Kono S, Narai H, Omori N, et al. Novel mutations of the GNE gene in distal myopathy with rimmed vacuoles presenting with very slow progression. Case Rep Neurol. 2012;4:120–5.
15. Malm C, Sjödin TL, Sjöberg B, Lenkei R, Renström P, Lundberg IE, et al. Leukocytes, cytokines, growth factors and hormones in human skeletal muscle and blood after uphill or downhill running. J Physiol. 2004;556:983–1000.
16. Zatz M, Rapaport D, Vainzof M, Passos-Bueno MR, Bortolini ER, Pavanello Rde C, et al. Serum creatine-kinase (CK) and pyruvate-kinase (PK) activities in duchenne (DMD) as compared with becker (BMD) muscular dystrophy. J Neurol Sci. 1991;102:190–6.
17. Cacchiarelli D, Legnini I, Martone J, Cazzella V, D'Amico A, Bertini E, et al. miRNAs as serum biomarkers for Duchenne muscular dystrophy. EMBO Mol Med. 2011;3:258–65.
18. Mizuno H, Nakamura A, Aoki Y, Ito N, Kishi S, Yamamoto K, et al. Identification of muscle-specific microRNAs in serum of muscular dystrophy animal models: promising novel blood-based markers for muscular dystrophy. PLoS ONE. 2011;6:e18388.
19. Jia Y, Suzuki N, Yamamoto M, Gassmann M, Noguchi CT. Endogenous erythropoietin signaling facilitates skeletal muscle repair and recovery following pharmacologically induced damage. FASEB J. 2012;26:2847–58.
20. Couteaux R, Mira JC, d'Albis A. Regeneration of muscles after cardiotoxin injury I. Cytological aspects. Biol Cell. 1988;62:171–82.
21. Roberts TC, Godfrey C, McClorey G, Vader P, Briggs D, Gardiner C, et al. Extracellular microRNAs are dynamic non-vesicular biomarkers of muscle turnover. Nucleic Acid Res. 2013;41:9500–13.
22. Forterre A, Jalabert A, Chikh K, Pesenti S, Euthine V, Granjon A, et al. Myotube-derived exosomal miRNAs downregulate Sirtuin1 in myoblasts during muscle cell differentiation. Cell Cycle. 2014;13:78–89.
23. Hudson MB, Woodworth-Hobbs ME, Zheng B, Rahnert JA, Blount MA, Gooch JL, et al. miR-23a is decreased during muscle atrophy by a mechanism that includes calcineurin signaling and exosome-mediated export. Am J Physiol Cell Physiol. 2014;306:C551–8.
24. Liu N, Williams AH, Maxeiner JM, Bezprozvannaya S, Shelton JM, Richardson JA, et al. microRNA-206 promotes skeletal muscle regeneration and delays progression of Duchenne muscular dystrophy in mice. J Clin Invest. 2012;122:2054–65.

Free Radical Biology and Medicine 82 (2015) 122–136

Contents lists available at ScienceDirect

Free Radical Biology and Medicine

journal homepage: www.elsevier.com/locate/freeradbiomed

Original Contribution

Low intensity training of *mdx* mice reduces carbonylation and increases expression levels of proteins involved in energy metabolism and muscle contraction

Janek Hyzewicz, Jun Tanihata, Mutsuki Kuraoka, Naoki Ito, Yuko Miyagoe-Suzuki, Shin'ichi Takeda *

Department of Molecular Therapy, National Institute of Neuroscience, National Center of Neurology and Psychiatry, 4-1-1 Ogawa-higashi, Kodaira, Tokyo 187-8502, Japan

ARTICLE INFO

Article history:
Received 19 August 2014
Received in revised form
22 January 2015
Accepted 23 January 2015
Available online 4 February 2015

Keywords:
mdx mouse
Oxidative stress
Proteomic
Exercise
Skeletal muscle
Blue Native PAGE

ABSTRACT

High intensity training induces muscle damage in dystrophin-deficient *mdx* mice, an animal model for Duchenne muscular dystrophy. However, low intensity training (LIT) rescues the *mdx* phenotype and even reduces the level of protein carbonylation, a marker of oxidative damage. Until now, beneficial effects of LIT were mainly assessed at the physiological level. We investigated the effects of LIT at the molecular level on 8-week-old wild-type and *mdx* muscle using 2D Western blot and protein–protein interaction analysis. We found that the fast isoforms of troponin T and myosin binding protein C as well as glycogen phosphorylase were overcarbonylated and downregulated in *mdx* muscle. Some of the mitochondrial enzymes of the citric acid cycle were overcarbonylated, whereas some proteins of the respiratory chain were downregulated. Of functional importance, ATP synthase was only partially assembled, as revealed by Blue Native PAGE analysis. LIT decreased the carbonylation level and increased the expression of fast isoforms of troponin T and of myosin binding protein C, and glycogen phosphorylase. In addition, it increased the expression of aconitate hydratase and NADH dehydrogenase, and fully restored the ATP synthase complex. Our study demonstrates that the benefits of LIT are associated with lowered oxidative damage as revealed by carbonylation and higher expression of proteins involved in energy metabolism and muscle contraction. Potentially, these results will help to design therapies for DMD based on exercise mimicking drugs.

Introduction

Duchenne muscular dystrophy (DMD) is a lethal inherited neuromuscular disease caused by mutations in the *DMD* gene. A lack of dystrophin in skeletal muscle of DMD patients causes injuries through multiple pathogenic mechanisms, including mechanical weakening of the sarcolemma [1], inappropriate calcium flux [2], and increased oxidative stress [3].

Physical exercise causes mechanical stress, calcium flux, and oxidative stress in skeletal muscle [4] and thereby, high intensity training (forced, above fatigue threshold, and damaging) was used to injure muscles of dystrophin-deficient *mdx* mice, an animal model for DMD [5]. In contrast, low intensity training (LIT) (voluntary, short, and nondamaging) rescued *mdx* mice phenotypes. Improved force output, tetanic tension, and endurance capacities of *mdx* muscles were reported after low intensity swimming [6] and running [7,8]. Another study also showed a reduction of markers of oxidative stress in *mdx* gastrocnemius after low intensity running [9]. This effect of low intensity training was especially interesting, given the fact that oxidative stress was thought to play a role in exacerbation of DMD pathology [10].

Oxidative stress is defined as "an imbalance between oxidants and antioxidants in favor of the oxidants, leading to a disruption of redox signaling and control, and/or molecular damages" [11]. One of the most common types of oxidative modification is protein carbonylation, the introduction of carbonyl groups (C=O) in a protein [12]. We chose protein carbonylation as a marker of oxidative stress, because it is a reliable indicator of oxidative damages [13], suitable for proteomic analysis [14] and commonly used on *mdx* muscle [15,16]. Studies reported an abnormal oxidative stress in skeletal muscle of DMD patients and *mdx* mice [17,18]. Indeed, myofibers lacking dystrophin were highly susceptible to oxidant-induced injury [19] and thus, the

Abbreviations: 2D-PAGE, two dimensional polyacrylamide gel electrophoresis; BN-PAGE, Blue Native polyacrylamide gel electrophoresis; Co-IP, coimmunoprecipitation; DMD, Duchenne muscular dystrophy; DNPH, 2,4-dinitrophenylhydrazine; IEF, isoelectric focusing; LIT, low intensity training; GP, glycogen phosphorylase; MyBP-C, myosin binding protein C

* Corresponding author. Fax: +81 42 346 1750.
E-mail address: takeda@ncnp.go.jp (S. Takeda).

http://dx.doi.org/10.1016/j.freeradbiomed.2015.01.023

protein carbonylation level correlated with the degree of the disease [20]. In the absence of dystrophin, oxidative stress acts together with mechanical stress to worsen fiber damage [17].

In healthy muscle, physical exercise leads to a production of oxidants through the mitochondrial electron transport chain [21], sarcolemmal NADPH oxidase [22], and xanthine oxidase [23]. These oxidants participate in cell signaling through MAPK and JNK pathways [24], leading to muscle adaptation to training (for example, overexpression of mitochondrial enzymes) [25]. In *mdx* muscle, this production of oxidants is known to be abnormally amplified by a mitochondrial overload of Ca^{2+} [4] and an overactivation of the NADPH oxidase 2 [26]. As a consequence, MAPK and JNK signaling pathways have been shown to be altered [27].

We aimed to clarify how low intensity training improved *mdx* phenotypes despite an abnormal oxidative environment. Thus, we investigated, for the first time, the effects of low intensity training at the protein level. Protein downregulation has been previously reported in nonexercised *mdx* muscle [28]. Our first hypothesis was that overcarbonylated proteins in nonexercised *mdx* muscle would be also downregulated and would lose protein-protein interactions, since carbonyl adducts target proteins for proteasomal degradation [29] and potentially affect interactions between proteins [30]. Our second hypothesis was that low intensity training would rescue proteins impaired in nonexercised *mdx* muscle, because physical exercise upregulates antioxidant defenses [31] and stimulates muscle plasticity [32].

We performed an extensive proteomic study on gastrocnemius muscle of 8-week-old *mdx* mice using 2D electrophoresis, known for its excellent reproducibility [33] and its reliability in skeletal muscle protein analysis [21,34,35]. Carbonylated proteins were detected by 2D carbonylated protein Western blot, protein expression was measured by 2D-PAGE, and protein–protein interactions were assessed by Blue Native PAGE (BN-PAGE). Detected proteins were identified by mass spectrometry.

Here we show that in nonexercised *mdx* muscle, proteins from muscle contraction and glycogen metabolism were both overcarbonylated and downregulated. Also, two complexes composed of ATP synthase subunits were absent. In exercised *mdx* muscle, these proteins were less carbonylated and higher expressed, and the ATP synthase complex was restored. Specifically, expression of the slow isoforms of the muscle contraction proteins troponin T and myosin binding protein C (MyBP-C) was increased, while carbonylation and expression level of fast isoforms were restored to the level of exercised wild-type mice. Thus, we demonstrated that the benefits of LIT are associated with lower carbonylation and higher expression of proteins involved in energy metabolism and muscle contraction.

Materials and methods

Animals

Eight-week-old male *mdx* mice with C57BL/6 background and age-matched wild-type C57BL/6 male control mice were used in this study. All experimental protocols were approved by The Experimental Animal Care and Use Committee of the National Institute of Neuroscience, National Center of Neurology and Psychiatry (NCNP), Tokyo, Japan.

Low intensity training protocol

Mice underwent training when they reached 4 weeks old. According to previously described protocol [7], mice were introduced into a tank filled with water (maintained at 35 ± 1 °C) to a depth enough to allow them to swim. Animals completed a 4 week program, in which they exercised 4 days (Monday, Tuesday, Thursday, and Friday) in a week for 30 min per day. A rest was given the three other days. Animals were not forced to move and were free to stand by at will.

Physiological tests

For serum creatine kinase measurement, blood was taken from the tail artery and centrifuged at 3000g for 10 min. Creatine kinase was assayed with the Fuji Drychem system (Fuji Film Medical Co. Ltd, Tokyo, Japan) as previously described [36]. Grip strength of both forelimb and hind limb was assessed by a grip strength meter, to determine the effects of LIT on whole body musculature of the mice (MK-380M; Muromachi Kikai), as previously described [37].

Then, mice were sacrificed by cervical dislocation. Gastrocnemius muscles were dissected and flash-frozen for histology or stored at −80 °C for 2D electrophoresis, Western blot, and PCR analysis. We assessed the effects of LIT on gastrocnemius, a muscle predominantly activated during swimming exercise [38].

Hematoxylin and eosin (H&E) staining

Frozen gastrocnemius muscles were cut in 20 μm sections using a cryostat and stained using Harris H&E as previously described [37].

Protein sample preparation for 1D and 2D carbonylated protein Western blot or Western blot

Muscles were homogenized using a lysis buffer made of 8 M urea, 2 M thiourea, 4% (w/v) Chaps, 12 μl/ml Destreak (Invitrogen, Carlsbad, CA), and clarified by centrifugation. Protein concentration was determined by the Bradford method (Bio-Rad Life Science, Hercules, CA). Twenty micrograms of proteins were prepared according to the Millipore protein oxidation detection kit instructions for 1D carbonylated protein Western blot, or prepared for classical Western blot. For 2D carbonylated protein Western blot, 200 μg of proteins was diluted in a rehydration solution made of 8 M urea, 1 M thiourea, 2% (w/v) Chaps, 12 μl/ml Deastreak, 0.5% (v/v), IPG buffer (GE Healthcare, Tokyo, Japan), and 0.001% of Coomassie blue, for a final volume of 250 μl. Then, they were charged on 13 cm (carbonylated protein Western blot) IGP strips, pH 3–10 Non Linear, overnight at room temperature, and isofocused with IPGphor (GE Healthcare) at the following profile: 500 V at 500 V/h, 1000 V in gradient at 1000 V/h, 6000 V in gradient at 20,000 V/h, and 6000 V at 12,000 V/h. After that, strips were prepared as previously described [39]. Briefly, strips were incubated for 20 min in derivatization solution (10 mM DNPH, 2 M HCl) and washed for 10 and 30 min in neutralizing solution (2 M Tris, 30% (v/v) glycerol).

Electrophoresis and immunoblotting

Proteins were separated in SDS-PAGE gels (12% (v/v) polyacrylamide). For each condition, two gels were performed in parallel, one for colloidal blue staining of total proteins and the other one for electroblotting onto nitrocellulose membrane. After blocking, membranes were incubated with corresponding antibody (see supplementary material and methods) and developed using an Amersham ECL Plus Western blotting detection system. Films were digitized with Epson GT-X900 scan and densitometric analyses were performed using ImageJ software (developed by U.S. National Institutes of Health and available at http://imagej.nih.gov/ij/).

Protein sample preparation for Blue Native PAGE

For sample preparation, muscles were homogenized using a BN-lysis buffer (20 mM Tris-HCl, 137 mM NaCl, 0.2 mM EDTA,

10% (v/v) glycerol, protease inhibitor cocktail, 1% digitonin, adjusted to pH 7), as previously described [40] and centrifuged at 600g at 4 °C for 10 min to remove tissue debris. Supernatants were dialyzed overnight in a 10,000 MWCO dialysis cassette (Thermo Fisher Scientific Inc., Waltham, MA, USA) with 0.3% digitonin in BN-lysis buffer. Protein quantification was performed using the Bradford method (Bio-Rad protein assay) with BSA as a standard.

Blue Native PAGE

Samples of 200 μg of proteins were homogenized using a NativePAGE sample preparation kit (Invitrogen, Carlsbad, CA, USA), according to the instructions of the manufacturer, but without digitonin. Proteins were separated in a first dimension in a 4–15% acrylamide-bisacrylamide gel, incubated for 15 min at room temperature in SDS sample buffer made of 12.5 mM Tris, 4% (w/v) SDS, 20% (w/v) glycerol, and 0.02% (w/v) bromophenol blue, reincubated for 20 min in the same SDS sample buffer, boiled at 100 °C, and then separated in second dimension in 12% (v/v) polyacrylamide SDS-PAGE gel and stained by Coomassie blue.

Data acquisition and analysis of Western blots and Blue Native PAGE

For 2D carbonylated protein Western blot, spots were quantified by densitometry in nitrocellulose membranes using ImageJ software. Spots were normalized with corresponding Coomassie blue values. These are reported in Supplementary Table 2.

In-gel digestion, mass spectrometry protein identification, database searches

All the following step were performed by the "Plateforme de protéomique de l'Université Paris-Descartes 3P5" (France) and described in detail in the supplementary material and methods. The identity of detected proteins is reported in Supplementary Table 1.

Coimmunoprecipitation

Coimmunoprecipitation was performed using Novex Dynabeads protein G immunoprecipitation kit (Life Technologies Japan Ltd., Tokyo, Japan) according to the manufacturer's instructions. Corresponding antibody was used to detect the prey protein in Western blotting, depending on the bait antibody [41].

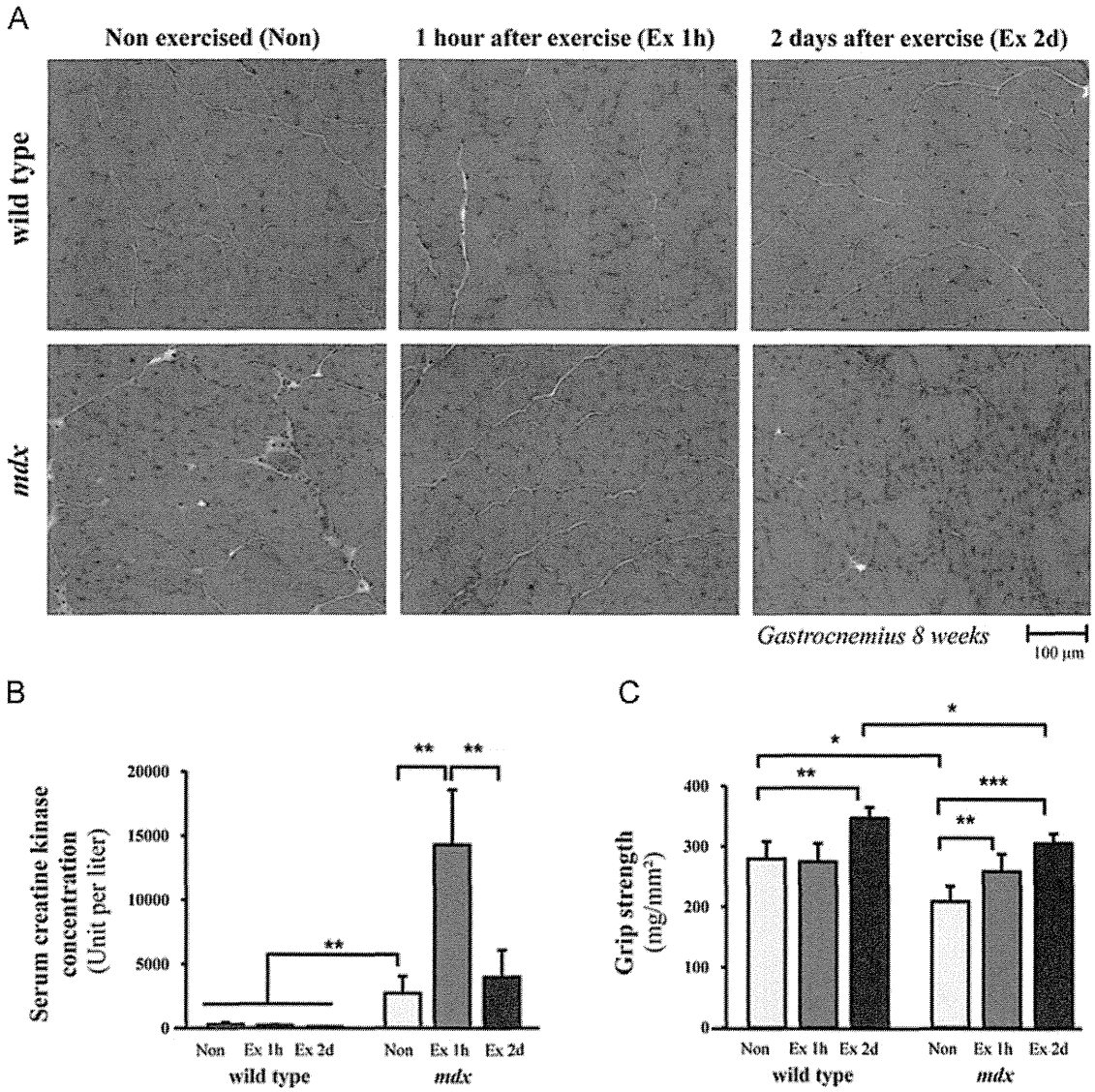

Fig. 1. Profile of 8-week-old wild-type and *mdx* mice after 4 weeks of swimming exercise. H&E staining of gastrocnemius muscle (A), serum creatine kinase concentration (B), and grip strength (C) from 8-week-old wild-type and *mdx* mice, nonexercised (Non) or after 4 weeks of swimming exercise, 1 h (Ex 1h) or 2 days (Ex 2d) after the last session. $^{*}P < 0.05$, $^{**}P < 0.01$, $^{***}P < 0.001$ means a significant difference between two groups. $n = 4$ to 6 per group. Scale bar represents 100 μm.

Sample preparation for PCR

Total RNA was extracted from muscles using TRIzol (Invitrogen). One microgram of total RNA template was used for PCR with a QuantiTect reverse transcription kit (Qiagen, Crawley, UK), according to the manufacturer's instructions. The cDNA product (1 μl) was then used as template for PCR in a 25 μl reaction solution with 0.125 unit of TaqDNA polymerase (Qiagen). The reaction mixture comprised 10X PCR

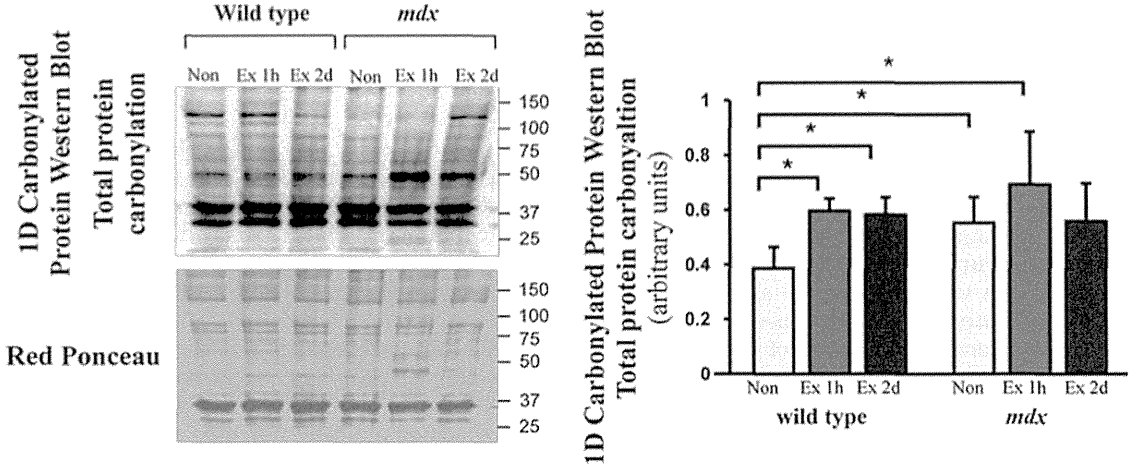

Fig. 2. Total protein carbonylation level in wild-type and *mdx* gastrocnemius muscle. Carbonylated proteins were detected by 1D carbonylated protein Western blot in gastrocnemius muscle of 8-week-old wild-type and *mdx* mice, nonexercised (Non) or after 4 weeks of swimming exercise, 1 h (Ex 1h) or 2 days (Ex 2d) after the last session. Ponceau red staining is shown as loading control. $^{*}P < 0.05$, $^{**}P < 0.01$, $^{***}P < 0.001$ means a significant difference between two groups. $n = 4$ to 6 per group.

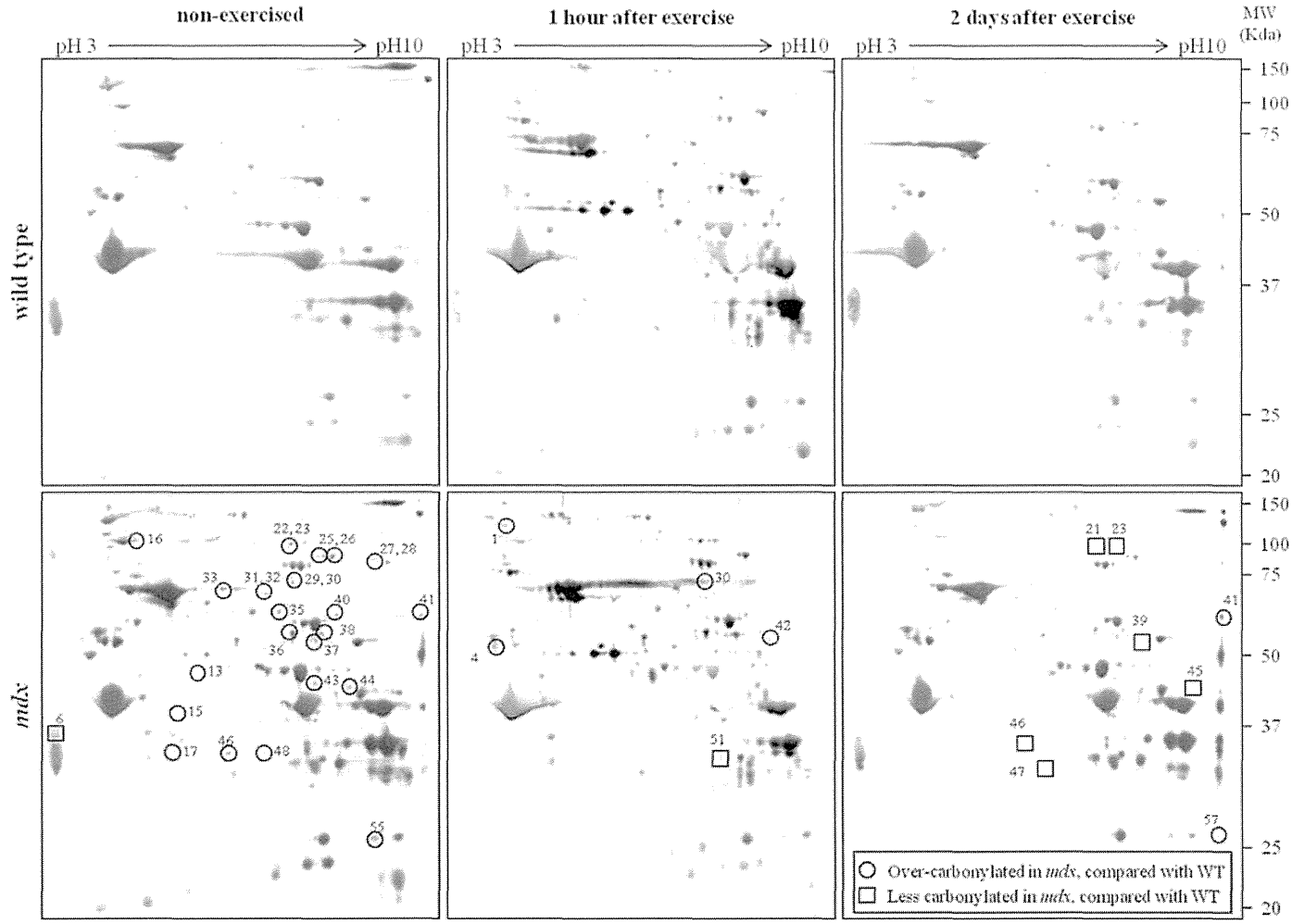

Fig. 3. Representative 2D carbonylated protein Western blot of gastrocnemius muscle from 8-week-old nonexercised and exercised wild-type and *mdx* mice. Proteins were separated by IEF and carbonylated proteins were derivatized with DNPH in the strip (13 cm, 3–10 NL). Second dimension was performed in 12% acrylamide SDS PAGE. Protein carbonylation was compared two by two between wild-type and *mdx* mice for each condition: nonexercised, 1 h after the last swimming session or 2 days after. ○ represents overcarbonylated spots in *mdx* in comparison with wild-type. □ represents less carbonylated spots in *mdx* in comparison with wild-type. Numbers indicate the spots identified by MS (Supplementary Table 1A) and listed in Table 1. For each experiment, gastrocnemius muscles from five different mice were pooled and electrophoresis was performed in triplicate.

buffer (Roche, Basel, Switzerland), 10 mmol/L of each dNTP (Qiagen), and 10 μmol/L of each primer. The primers for PCR were synthesized by Operon Biotechnologies (Tokyo, Japan) and are listed in Supplementary Table S2. The cycling conditions were 95 °C for 4 min, 35 cycles at 94 °C for 1 min, 60 °C for 1 min, 72 °C for 1 min, and finally 72 °C for 7 min. The intensity of PCR bands was analyzed by ImageJ software. Relative gene expression levels were normalized to those of 18S rRNA.

Statistics

Values are reported as mean ± SD (standard deviation). The number of mice analyzed per group is shown in the figure legends. Statistically significant differences between two groups were determined by Student's *t* test, with a *P* value of $P < 0.05$ considered significant. Statistically significant differences between more than two groups were determined by ANOVA test followed by Tukey's range test, a *P* value of $P < 0.05$ was considered significant for ANOVA test, and a result superior to the minimum significant difference was considered significant for the Turkey test.

Results

Effects of low intensity swimming on 8-week-old mice

We assessed the effects of swimming exercise on wild-type and *mdx* muscle. No changes were observed in sections from gastrocnemius muscle after 1 h past the last session of 4 weeks of swimming (Fig. 1A), even though creatine kinase levels were significantly increased ($P < 0.01$) at this time. Creatine kinase levels returned to nonexercised values after 2 days (Fig. 1B). Of note, exercise led to an increase in grip strength of wild-type and *mdx* mice (Fig. 1C).

Total protein carbonylation level after low intensity swimming

The level of oxidative stress in muscle was quantified by measurement of protein carbonylation [12]. Carbonyls groups were derivatized into their DNP adducts using DNPH and these were detected by carbonylated protein Western blot. In wild-type muscle, total protein carbonylation levels increased 1 h after exercise ($P < 0.05$) and remained elevated 2 days after, as observed in previous studies [42]. Interestingly, in *mdx* muscle, total protein carbonylation level was not significantly different after exercise (Fig. 2).

Influence of low intensity training on the proteome of gastrocnemius muscle

Proteomic analysis of wild-type and *mdx* gastrocnemius muscles was performed by 2D carbonylated protein Western blot to detect alterations in protein carbonylation (Fig. 3), 2D-PAGE to examine protein expression (Fig. 4), and BN-PAGE to detect protein–protein

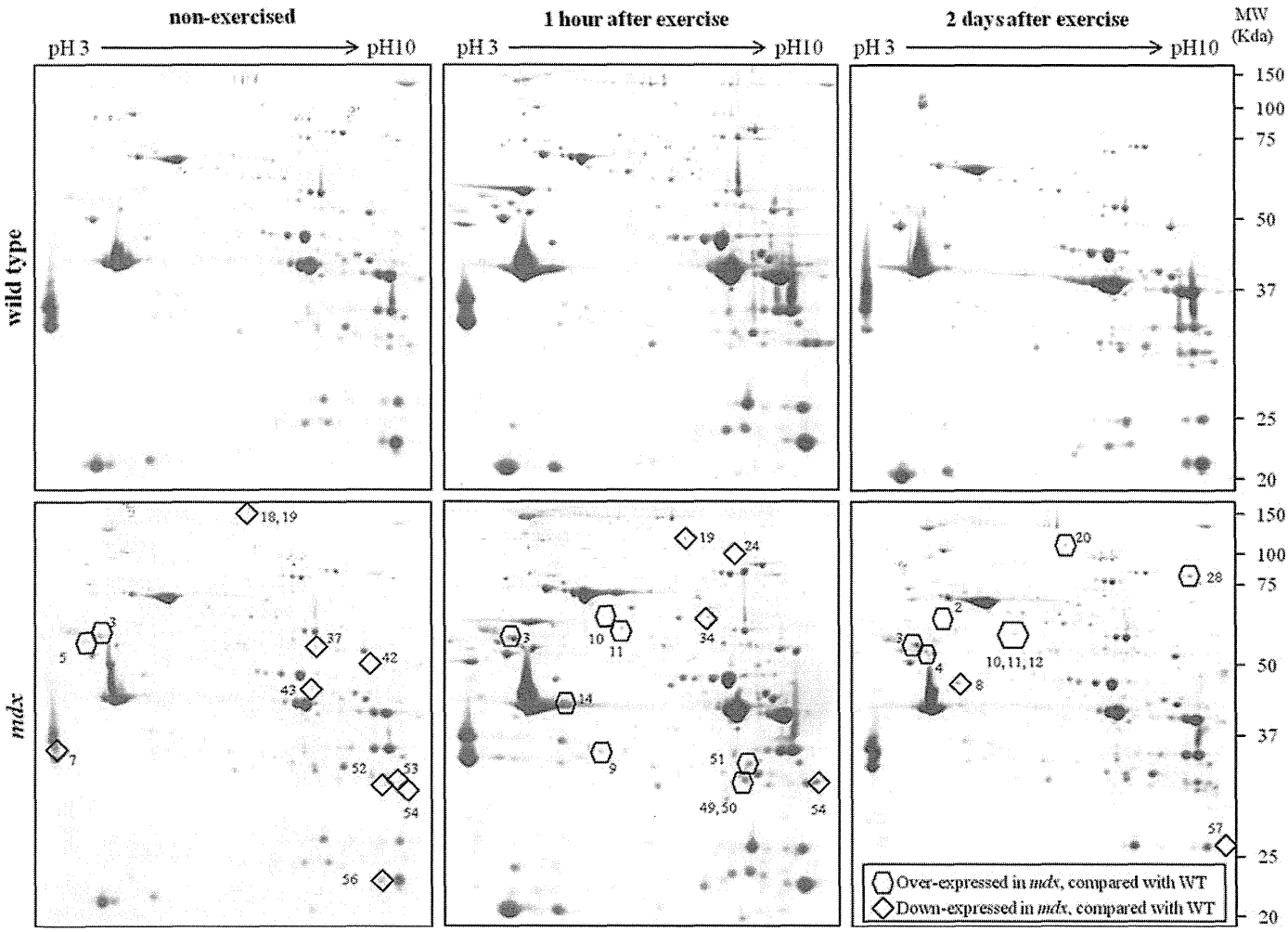

Fig. 4. Representative Coomassie blue staining of gastrocnemius muscle from 8-week-old nonexercised and exercised wild-type and *mdx* mice. Corresponding Coomassie blue gels related to Fig. 3. Protein expression was compared two by two between wild-type and *mdx* mice. ○ represents overexpressed spots in *mdx* in comparison with wild type. ◇ represents downregulated spots in *mdx* in comparison with wild-type muscle. Numbers indicate spots identified by MS (Supplementary Table 1A) and listed in Table 2.

interaction (Fig. 5). In a first step, we compared nonexercised wild-type muscle with nonexercised *mdx* muscle and in a second one, nonexercised muscle with exercised ones in both types of mice. Spots displaying a change of at least 50% were selected for mass spectrometrical identification. A total of 76 spots were identified (Supplementary Table 1) and grouped by categories according to the SwissProt/UniProtKB data base (Tables 1–4).

Proteome of 8-week-old nonexercised wild-type and mdx gastrocnemius muscle

Overcarbonylated proteins in *mdx* muscle were mainly involved in the citric acid cycle, for example, succinate dehydrogenase, aconitate hydratase, in muscle contraction such as the fast isoforms of troponin T and MyBP-C, in glycogen metabolism, such as glycogen phosphorylase (GP) and glycolysis and in cytoskeleton (Table 1A and Fig. 3).

Downregulated proteins were involved in the respiratory chain, muscle contraction, glycogen metabolism, and the stress response. Interestingly, fast isoforms of troponin T and MyBP-C and glycogen phosphorylase were both carbonylated and downregulated. Overexpressed proteins were involved in glycolysis and in the microtubular cytoskeleton (Tables 2 and 3A and Figs. 4 and 5).

Protein–protein interaction analysis by BN-PAGE revealed the absence of ATP synthase subunits α and β in *mdx* muscle (Table 3D and Fig. 5).

Proteome of nonexercised and exercised gastrocnemius in wild-type or mdx muscle

We compared nonexercised muscle with exercised muscle 2 days after the last swimming session (Table 4 and Figs. 3–5). In wild-type muscle, LIT increased protein carbonylation, but had little influence on protein expression. Proteins involved in the citric acid cycle, the fast isoforms of troponin T and MyBP-C, and UTP-glucose-1-phosphate uridylyl transferase were more carbonylated in exercised wild-type muscle (Fig. 3) as compared to control, whereas beta-enolase was overexpressed (Figs. 4 and 5).

In *mdx* muscle (Table 4 and Figs. 3–5), LIT decreased the carbonylation and enhanced the expression of specific proteins. While total protein carbonylation remained unchanged by exercise (Fig. 2), voltage-dependent anion-selective channel protein 1, fast isoforms of troponin T and MyBP-C, and phosphoglucomutase-1 were less carbonylated in exercised *mdx* muscle (Fig. 3). In contrast to wild-type muscle, LIT increased protein expression of some respiratory chain proteins, the fast isoforms of troponin T and

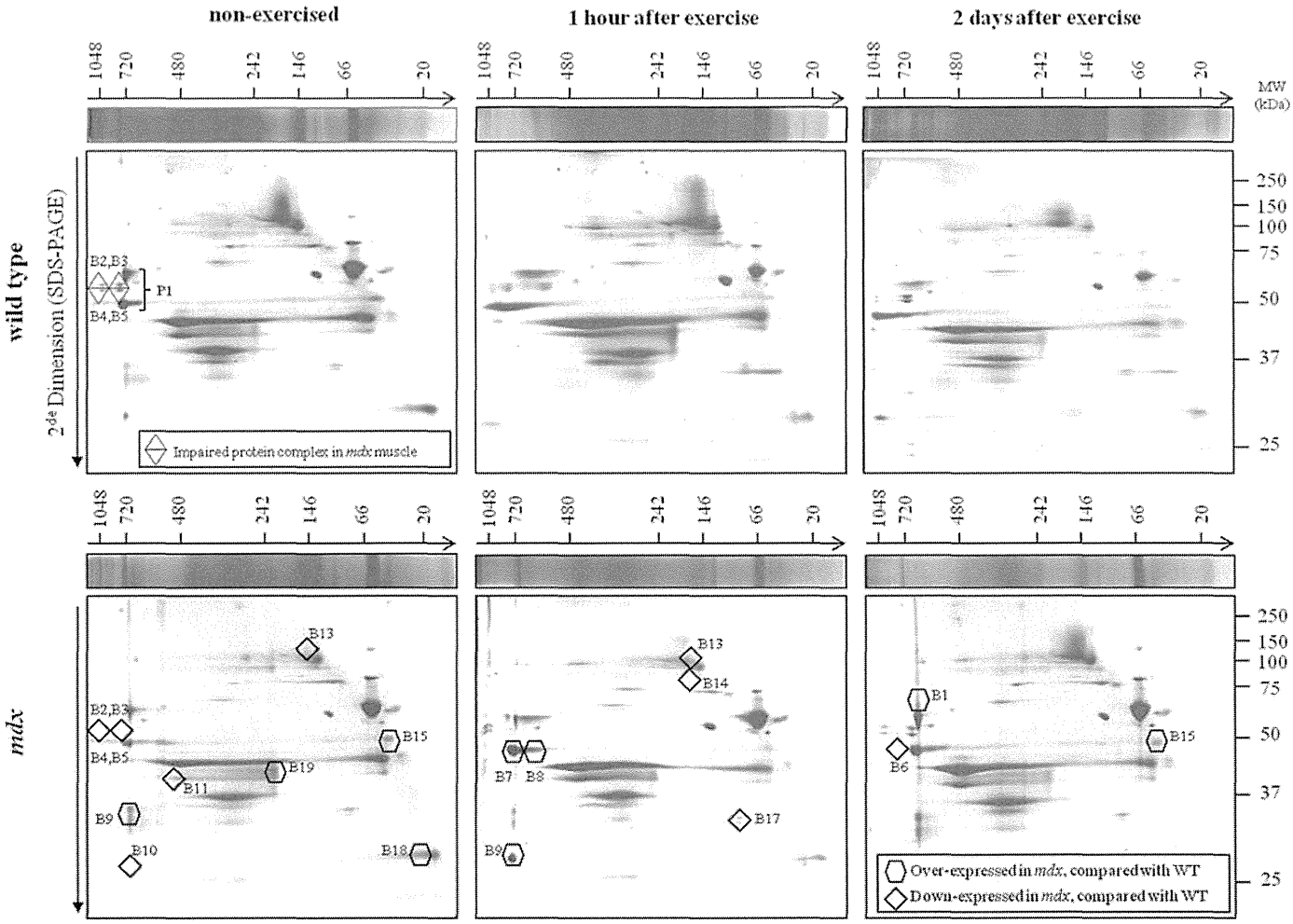

Fig. 5. Representative Blue Native PAGE of gastrocnemius muscle from 8-week-old nonexercised and exercised wild-type and *mdx* mice. Proteins were separated under nondenaturing conditions in 4–15% acrylamide-bisacrylamide gel. Second dimension was performed in 12% acrylamide SDS PAGE. ◇ represents the protein complexes present in wild-type, but absent in *mdx* gels. P numbers represent protein complexes listed in Table 3D. As for Fig. 3, protein expression was compared two by two between wild-type and *mdx* mice. ⬡ represents overexpressed spots in *mdx* in comparison with wild type. ◇ represents downregulated spots in *mdx* in comparison with wild type. B numbers indicate spots identified by MS (Supplementary Table 1B) and listed in Table 3. For each experiment, gastrocnemius muscles from five different mice were pooled and electrophoresis was performed in triplicate.

Table 1
Identity of proteins whose carbonylation differs in mdx gastrocnemius, in comparison with wild type.

Protein carbonylation in mdx muscle
(in comparison with wild type)

A. Nonexercised				B. Exercised, 1 h after the last session				C. Exercised, 2 days after the last session			
Spot No. [a]	Accession No. [b]	Protein name	Fold change [c]	Spot No. [a]	Accession No. [b]	Protein name	Fold change [c]	Spot No. [a]	Accession No. [b]	Protein name	Fold change [c]
↑ Mitochondria				↑ Mitochondria				↑ Muscle contraction			
29	Q8CAQ8	Mitochondrial inner membrane protein	20	30	Q8CAQ8	Mitochondrial inner membrane protein	5.26	57	P05977	Myosin light chain 1/3, skeletal muscle	Only mdx
30	Q8CAQ8	Mitochondrial inner membrane protein	14.29	42	Q91YT0	NADH dehydrogenase flavoprotein 1	3.85	41	Q9JIF9	Myotilin	Only mdx
31	Q8K2B3	Succinate dehydrogenase flavoprotein sub	14.29	Cytoskeleton				Others			
32	Q8K2B3	Succinate dehydrogenase flavoprotein sub	14.29	4	P31001	Desmin	3.13	57	O70250	Phosphoglycerate mutase 2	Only mdx
38	Q9D0K2	Succinyl-CoA:3-ketoacid coA transferase 1	14.29	Other				57	Q9CQA3	Succinate dehydrogenase iron-sulfur subunit	Only mdx
43	P35486	Pyruvate dehydrogenase E1 subunit alpha	7.69	1	P59242	Cingulin	3.23	↓ Mitochondria			
33	P13707	Glycerol-3-phosphate dehydrogenase	5	↓ Glycolysis				45	Q9DB77	Cytochrome b-c1 complex subunit 2	-6.06
25	Q99KI0	Aconitate hydratase, mitochondrial	4.76	51	P05064	Fructose-bisphosphate aldolase A	-3.72	39	Q03265	ATP synthase subunit alpha, mitochondrial	-3.07
26	Q99KI0	Aconitate hydratase, mitochondrial	4.35	51	P16858	Glyceraldehyde-3-phosphate dehydrogenase	-3.72	Glycogen metabolism			
36	O08749	Dihydrolipoyl dehydrogenase, mitochondrial	4.35					21	Q9WUB3	Glycogen phosphorylase, muscle form	-5.01
Muscle contraction								23	Q9WUB3	Glycogen phosphorylase, muscle form	-5.16
48	Q9QZ47	Troponin T, fast skeletal muscle	7.69					39	Q91ZJ5	UTP-glucose-1-phosphate uridylyltransferase	-3.07
16	Q5XKE0	Myosin-binding protein C, fast-type	5.56					Muscle contraction			
41	Q9JIF9	Myotilin	5					46	Q9QZ47	Troponin T, fast skeletal muscle	-3.31
46	Q9QZ47	Troponin T, fast skeletal muscle	5					Others			
Glycogen metabolism								47	P14152	Malate dehydrogenase, cytoplasmic	-7.27
35	Q9D0F9	Phosphoglucomutase-1	8.33					46	P07310	Creatine kinase M-type	-3.31
23	Q9WUB3	Glycogen phosphorylase, muscle form	7.69					39	P97384	Annexin A11	-3.07
22	Q9WUB3	Glycogen phosphorylase, muscle form	6.25								
37	Q91ZJ5	UTP-glucose-1-phosphate uridylyltransferase	6.25								
Glycolysis											
40	P52480	Pyruvate kinase isozymes M1/M2	33.33								
55	O70250	Phosphoglycerate mutase 2	7.69								
48	P21550	Beta-enolase	7.69								
13	P21550	Beta-enolase	4								
Cytoskeleton											
29	P48678	Prelamin-A/C	20								
31	O88342	WD repeat-containing protein 1	14.29								
15	P68033	Actin, alpha cardiac muscle 1	7.14								
28	Q9JKS4	LIM domain-binding protein 3	5								
27	Q9JKS4	LIM domain-binding protein 3	4.76								
17	P47753	F-actin-capping protein subunit alpha-1	4								

Others				
44	P07310	Creatine kinase M-type	10	
43	P62196	26S protease regulatory subunit 8	7.69	
48	P10518	Delta-aminolevulinic acid dehydratase	7.69	
↓ Muscle contraction				
6	P58774	Tropomyosin beta chain	- 5.60	

↑ Refer to proteins whose carbonylation is higher in *mdx* than in wild-type muscle.
↓ Refer to proteins whose carbonylation is lower in *mdx* than in wild-type muscle.
[a] Spots refer to annoted spots in Fig. 3.
[b] Accession number in UniProtKB/Swiss-prot.
[c] Fold change between mdx and wild-type values. A positive fold change means an increased value in mdx, a negative means a decreased value.

MyBP-C, UTP-glucose-1-phosphate uridylyltransferase, and carbonic anhydrase 3 (Figs. 4 and 5).

The difference in carbonylation levels between exercised wild-type and *mdx* muscles was reduced 1 h after the last session of LIT (Tables 1–3B) and 2 days later, ATP synthase subunit α, fast isoform of troponin T, and GP were less carbonylated in *mdx* muscle (Table 1C and Fig. 3). In contrast, expression of tubulin, vimentin, and associated proteins, as well as stress response proteins, was higher in exercised *mdx* muscle as of 1 h after the last session, and remained higher 2 days after (Tables 2 and 3B and Tables 2 and 3C; Figs. 4 and 5). Protein–protein interaction analysis showed that the two ATP synthase complexes absent in nonexercised *mdx* muscle were restored 1 h after LIT in *mdx* muscles (P1 in Table 3D and Fig. 5).

Validation of proteomic results by 1D carbonylated protein Western blot and Western blot

The above results point to differences in protein carbonylation and expression between wild-type and *mdx* muscles that are altered by LIT. To validate these results, we investigated these levels by coimmunoprecipitation (co-IP) followed by 1D carbonylated protein Western blot analysis. Two critical proteins were selected, namely GP (Fig. 4, spot 24; Fig. 5, spot B13), and the fast isoforms of MyBP-C (Fig. 4, spot 18).

We confirmed that GP (Fig. 6A) and MyBP-C (Fig. 6B) were significantly more carbonylated in nonexercised *mdx* muscle than in wild-type muscle, consistent with results shown in Table 1A. GP carbonylation was not significantly different between exercised wild-type and *mdx* muscles, 1 h after LIT (Table 1B) but significantly lower in exercised *mdx* muscle after 2 days (Table 1C). MyBP-C carbonylation was not significantly different between exercised wild-type and *mdx* muscles (Table 1B and C).

Expression was assessed by Western blot. We confirmed that GP (Fig. 7A) and MyBP-C (Fig. 7B) were downregulated in nonexercised *mdx* muscles, compared with nonexercised wild-type muscles, as found previously (Tables 2 and 3A). GP expression was lower in exercised *mdx* muscle than in wild-type muscle, 1 h after the last session (Table 2B) and after 2 days, it was similar in both types of mice (Table 3B). MyBP-C expression was not significantly different between exercised wild-type and *mdx* muscles (Table 2B and C). Altogether, results of co-IP and Western blot analysis were in accordance with the results of the proteomic study.

Increased expression of fast skeletal muscle isoforms in exercised mdx gastrocnemius muscle

Gastrocnemius muscle is composed of about 95% of fast type fibers [43]. Proteomic analysis revealed a lower expression of fast isoforms of troponin T and MYBP-C in *mdx* gastrocnemius muscle as compared to wild-type muscle (Table 2). Using Western blot analysis, we confirmed this result and showed that slow isoforms were more highly expressed in nonexercised *mdx*, compared with wild-type muscle (Fig. 7B). After swimming, a higher expression of slow isoforms was detected in both exercised wild-type and *mdx* muscles. Interestingly, in *mdx* muscle, we found a higher expression of fast isoforms, similar to the level of exercised wild-type muscle. This result showed that LIT stimulated the expression of slow type isoforms, and also restored the expression of fast isoforms in *mdx* muscle. These observations at the protein level were supported by a similar pattern at the mRNA level (Fig. 7C).

Discussion

Our study links, for the first time, alterations in protein carbonylation and expression levels, induced by low intensity

Table 2
Identity of proteins whose expression differs in mdx gastrocnemius, in comparison with wild type.

Protein expression in mdx muscle (2D-PAGE)
(in comparison with wild type)

A. Nonexercised				B. Exercised, 1 h after the last session				C. Exercised, 2 days after the last session			
Spot No. [a]	Accession No. [b]	Protein name	Fold change [c]	Spot No. [a]	Accession No. [b]	Protein name	Fold change [c]	Spot No. [a]	Accession No. [b]	Protein name	Fold change [c]
↑ Cytoskeleton				↑ Muscle contraction				↑ Cytoskeleton			
3	P05213	Tubulin alpha-1B chain	3.45	9	P58774	Tropomyosin beta chain	2.63	12	P11983	T-complex protein 1 subunit alpha	3.45
3	P20152	Vimentin	3.45	50	Q9QZ47	Troponin T, fast skeletal muscle	1.67	10	P11983	T-complex protein 1 subunit alpha	3.03
5	P68372	Tubulin beta-4B chain	1.79	49	Q9QZ47	Troponin T, fast skeletal muscle	1.54	10	P80316	T-complex protein 1 subunit epsilon	3.03
↓ Mitochondria				Glycolysis				4	P31001	Desmin	2.56
43	P35486	Pyruvate dehydrogenase E1 subunit alpha	-2.35	51	P05064	Fructose-bisphosphate aldolase A	2.86	28	Q9JKS4	LIM domain-binding protein 3	2.44
56	Q9DCS9	NADH dehydrogenase 1 β subcomplex sub 10	-2.21	51	P16858	Glyceraldehyde-3-phosphate dehydrogenase	2.86	3	P05213	Tubulin alpha-1B chain	1.82
42	Q91YT0	NADH dehydrogenase flavoprotein 1	-2.18	9	P21550	Beta-enolase	2.63	3	P20152	Vimentin	1.82
54	Q60932	Voltage-dependent anion-selective channel 1	-2.03	Cytoskeleton				Stress response			
Muscle contraction				10	P11983	T-complex protein 1 subunit alpha	2.17	11	P27773	Protein disulfide-isomerase A3	4.17
53	Q9QZ47	Troponin T, fast skeletal muscle	-2.78	10	P80316	T-complex protein 1 subunit epsilon	2.17	2	P63038	60 kDa heat shock protein, mitochondrial	2.86
56	Q9QZ47	Troponin I, fast skeletal muscle	-2.21	3	P05213	Tubulin alpha-1B chain	1.64	Others (cell cyke)			
18	Q5XKE0	Myosin-binding protein C, fast-type	-2.12	3	P20152	Vimentin	1.64	20	Q9WU78	Programmed cell death 6-interacting protein	4.17
54	Q9QZ47	Troponin T, fast skeletal muscle	-2.03	Stress response				↓ Mitochondria			
52	Q9QZ47	Troponin T, fast skeletal muscle	-1.74	11	P27773	Protein disulfide-isomerase A3	3.45	57	Q9CQA3	Succinate dehydrogenase iron-sulfur subunit	-2.93
7	P58771	Tropomyosin alpha-1 chain	-1.61	14	Q60854	Serpin B6	2.17	8	Q9CZ13	Cytochrome b-c1 complex subunit 1	-1.54
Glycogen metabolism				↓ Mitochondria				Glycolysis			
37	Q91ZJ5	UTP-glucose-1-phosphate uridylyltransferase	-1.71	54	Q60932	Voltage-dependent anion-selective channel 1	-2.29	57	O70250	Phosphoglycerate mutase 2	-2.93
Stress response				7	Q60597	2-oxoglutarate dehydrogenase	-1.67	Others			
43	P62196	26S protease regulatory subunit 8	-2.35	Muscle contraction				57	P05977	Myosin light chain 1/3. skeletal muscle isoform	-2.93
Others				54	Q9QZ47	Troponin T, fast skeletal muscle	-2.29	8	P60710	Actin. cytoplasmic 1	-1.54
43	Q9DCL9	Multifunctional protein ADE2	-2.35	Glycogen metabolism							
43	P07310	Creatine kinase M-type	-2.35	24	Q9WUB3	Glycogen phosphorylase, muscle form	-1.72				
				34	Q9D0F9	Phosphoglucomutase-1	-1.65				
				Stress response							
				24	P58252	Elongation factor 2	-1.72				

↑ Refer to proteins whose expression is higher in *mdx* than in wild-type muscle.
↓Refer to proteins whose expression is lower in *mdx* than in wild-type muscle.

[a] Spots refer to annoted spots in Fig. 4.
[b] Accession number in UniProtKB/Swiss-prot.
[c] Fold change between mdx and wild-type values. A positive fold change means an increased value in mdx, a negative means a decreased value.

training at the molecular level in muscle of *mdx* mice. We hypothesized first that overcarbonylated proteins in *mdx* muscle would also be downregulated and that protein–protein interactions would be lost. We also thought that LIT would rescue these changes, rendering LIT a physiotherapeutic approach to treatment.

In agreement with our first hypothesis, we found that proteins involved in muscle contraction and glycogen metabolism were both overcarbonylated and downregulated in nonexercised *mdx* muscle. However, this was not associated with a loss of protein–protein interactions.

Table 3
Identity of proteins whose expression and protein-protein interactions differs in *mdx* gastrocnemius, in comparison with wild type.

Protein expression in mdx muscle (BN-PAGE)
(in comparison with wild type)

A. Nonexercised

	Spot No. [a]	Accession No. [b]	Protein name	Fold change [c]
↑	Glycolysis			
	B9	P06151	L-lactate dehydrogenase A chain	2.56
	B15	P21550	Beta-enolase	1.75
	B19	P05064	Fructose-bisphosphate aldolase A	1.75
	Others			
	B19	P07310	Creatine kinase M-type	1.75
	B16	P07310	Creatine kinase M-type	1.64
↓	Mitochondria			
	B5	P56480	ATP synthase subunit beta, mitochondrial	-3.72
	B4	Q03265	ATP synthase subunit alpha, mitochondrial	-3.26
	B3	P56480	ATP synthase subunit beta, mitochondrial	-2.57
	B2	Q03265	ATP synthase subunit alpha, mitochondrial	-2.42
	Glycogen metabolism			
	B13	Q9WUB3	*Glycogen phosphorylase*, muscle form	-1.66
	Stress response			
	B10	P16015	Carbonic anhydrase 3	-3.9
	Others			
	B11	P07310	Creatine kinase M-type	-2.02
	B13	Q8R429	Sarco/endoplasmic reticulum calcium ATPase 1	-1.66

B. Exercised, 1 h after the last session

	Spot No. [a]	Accession No. [b]	Protein name	Fold change [c]
↑	Mitochondria			
	B8	P55084	Trifunctional enzyme subunit beta, mitochondrial	1.86
	Glycolysis			
	B8	P21550	Beta-enolase	1.86
	B8	P05064	Fructose-bisphosphate aldolase A	1.86
	B7	P21550	Beta-enolase	1.81
↓	Mitochondria			
	B14	Q99KI0	Aconitate hydratase, mitochondrial	-3.36
	B17	Q60932	Voltage-dependent anion-selective channel prot 1	-1.59
	Glycogen metabolism			
	B13	Q9WUB3	Glycogen phosphorylase, muscle form	-1.72
	Stress response			
	B14	P07901	Heat shock protein HSP 90-alpha	-3.36
	Other			
	B13	Q8R429	Sarco/endoplasmic reticulum calcium ATPase 1	-1.72
	B17	P07310	Creatine kinase M-type	-1.59
	B17	P14152	Malate dehydrogenase, cytoplasmic	-1.59

C. Exercised, 2 days after the last session

	Spot No. [a]	Accession No. [b]	Protein name	Fold change [c]
↑	Glycolysis			
	B15	P21550	Beta-enolase	1.59
	B1	P52480	Pyruvate kinase isozymes M1/M2	1.54
↓	Glycolysis			
	B6	P21550	Beta-enolase	-1.51

D. Identity of the proteins which compose the complexes absents in nonexercised *mdx* muscle

Spot No. [a]	Accession No. [b]	Protein name
P1 complexes		
B2	Q03265	ATP synthase subunit alpha, mitochondrial
B3	P56480	ATP synthase subunit beta, mitochondrial
B4	Q03265	ATP synthase subunit alpha, mitochondrial
B5	P56480	ATP synthase subunit beta, mitochondrial

↑Refer to proteins whose expression is higher in *mdx* than in wild-type muscle.
↓Refer to proteins whose expression is lower in *mdx* than in wild-type muscle.

[a] Spots refer to annoted spots in Fig. 5.
[b] Accession number in UniProtKB/Swiss-prot.
[c] Fold change between mdx and wild-type values. A positive fold change means an increased value in mdx, a negative means a decreased value.

Furthermore, we found that LIT rescued, at least in part, *mdx* muscle at the protein level, consistent with our second hypothesis. Specifically, proteins from mitochondria, muscle contraction, and glycogen metabolism, highly carbonylated and downregulated in nonexercised *mdx* muscle, were less carbonylated and highly expressed after LIT. LIT of *mdx* mice also restored carbonylation and expression levels of fast isoforms of troponin T and MyBP-C at the level of exercised wild-type muscle, while expression of slow isoforms increased, also consistent with our second hypothesis.

Protein carbonylation in skeletal muscle of nonexercised mdx mice

Elevated total protein carbonylation levels have been reported in muscle of *mdx* mice and DMD patients [17,20]. However, the targets